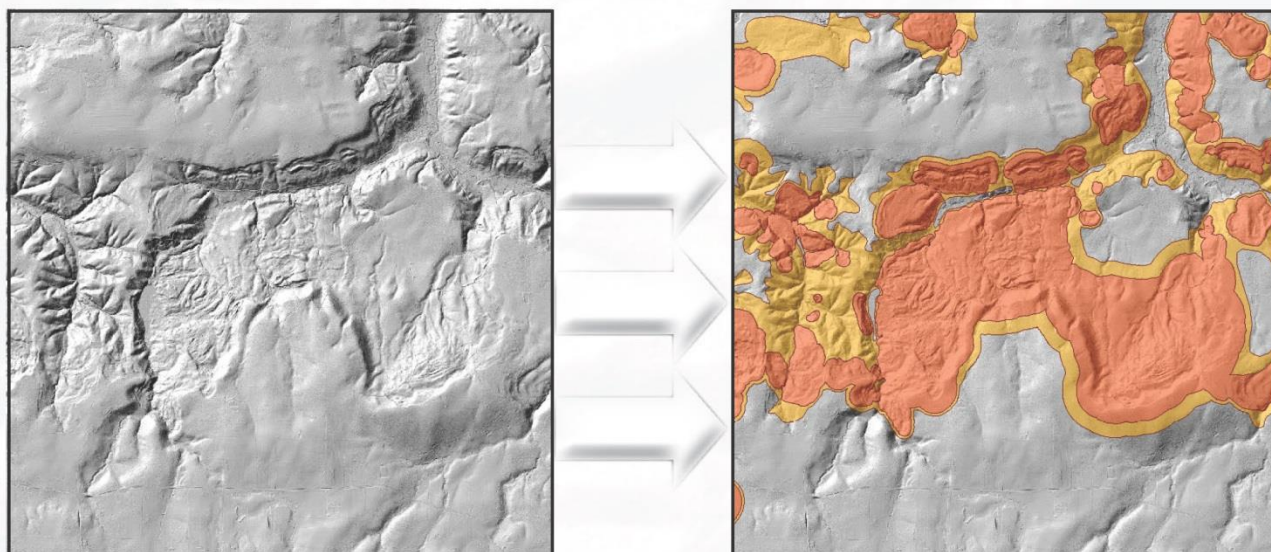# PROTOCOL FOR DEEP LANDSLIDE SUSCEPTIBILITY MAPPING

by William J. Burns and Katherine A. Mickelson

SPECIAL PAPER 48
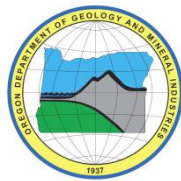
2016

State of Oregon
Oregon Department of Geology and Mineral Industries
Brad Avy, State Geologist

SPECIAL PAPER 48

PROTOCOL FOR DEEP LANDSLIDE SUSCEPTIBILITY MAPPING

by William J. Burns[1] and Katherine A. Mickelson[2]

2016

[1]Oregon Department of Geology and Mineral Industries, 800 NW Oregon Street, Suite 965, Portland, Oregon 97232
[2]Formerly with Oregon Department of Geology and Mineral Industries, 800 NW Oregon Street, Suite 965, Portland, Oregon 97232

DISCLAIMER

TABLE OF CONTENTS

LIST OF FIGURES

LIST OF TABLES

1.0 REPORT SUMMARY

Landslides are one of the most significant natural hazards in Oregon and cause millions of dollars in damage annually. Identifying areas susceptible to landslides is a critical step in reducing landslide risk. This paper describes the protocol used by the Oregon Department of Geology and Mineral Industries (DOGAMI) to develop standardized deep-landslide susceptibility maps. By identifying areas prone to deep landsliding, this protocol and products produced by following this protocol can be used to help Oregon communities become more resilient to impacts of landslide hazards.

The deep-landslide susceptibility map protocol described here begins with an existing landslide inventory data set to which are applied several types of buffers as well as factors derived from an engineering geologic map, a slope map, and an aspect map, to in order to define three relative deep-landslide susceptibility zones:

- High susceptibility zone
  - Inventory: landslide deposit polygons
  - Inventory: head scarp-flank polygons
  - Head scarp-flank polygon buffers
- Moderate susceptibility zone
  - Minimal moderate zone
  - Combination of four factors
    - Susceptible geologic units
    - Susceptible geologic contacts
    - Susceptible slopes in each engineering geologic unit polygon
    - Preferred direction of movement in each engineering geologic unit polygon
- Low susceptibility zone
  - Areas not identified in the high or moderate zones

The protocol also provides a map template for producing a standardized deep-landslide susceptibility map at a scale of 1:8,000, tiled by quarters of U.S. Geological Survey (USGS) 7.5 minute quadrangles.

2.0 INTRODUCTION

Landslides are among of the most devastating natural disasters. Worldwide, they cause billions of dollars in property damage and thousands of deaths every year (Hong and others, 2007). Landslides in the United States cause an average of 25–50 deaths and over $2 billion in economic losses annually (Turner and Schuster, 1996; Spiker and Gori, 2003).

Large deep landslides are a significant hazard in the Pacific Northwest. As an example, on March 22, 2014, the Oso landslide in Snohomish County, Washington, claimed the lives of 43 people, making it the deadliest landslide in United States history (Keaton and others, 2014). Keaton and others (2014) concluded that this landslide was a reactivation of an existing deep landslide known as the Hazel Landslide; they estimated that the slide was several hundred feet (60–90 m) thick and traveled 0.6 mi (1 km) across the valley floor. (**Figure 2.1**).

Figure 2.1. The March 22, 2014, Oso landslide, Snohomish County, Washington. The slide traveled 0.6 mi (1 km) across the valley floor. Photograph by Mark Reid, USGS.

In Oregon, landslides pose significant threats to people and infrastructure. As population continues to expand and as development on landslide susceptible terrain increases, greater losses are likely to result (**Figure 2.2**).

Figure 2.2. Risk diagram displaying the overlap of the landslide hazard and the vulnerable population (modified after Wood, 2007).
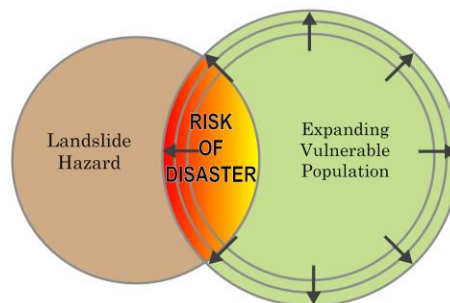
Most of Oregon's landslide damage has been associated with severe winter rainstorms. Direct landslide damage losses from these storms can exceed $100 million in direct damage (such as the February 1996 event) (Wang and others, 2002). However, landslides are also a chronic hazard in Oregon; annual average maintenance and repair costs for landslides in Oregon are estimated at over $10 million (Wang and others, 2002). In addition, many parts of Oregon are susceptible to landslides induced by earthquake shaking. Losses associated with sliding caused by moderate to large earthquakes are likely to be significant. Volcano-induced landslide hazards are also potential threats to parts of Oregon.

Geologists at the Oregon Department of Geology and Mineral Industries (DOGAMI) have begun systematically to map landslides in Oregon by using lidar and following the method described in DOGAMI Special Paper 42 (SP-42), Protocol for inventory mapping of landslide deposits from light detection and ranging (lidar) imagery (Burns and Madin, 2009a). The result of this mapping is a significantly improved landslide inventory for any particular area. A landslide inventory based on lidar-derived topographic data, and an engineering geologic map are the fundamental data sets used in this protocol to develop deep landslide susceptibility maps.

In 2012 Burns and others provided a method that uses infinite slope analysis to map shallow landslide susceptibility. However, Baum and others (2008, p. 7) concluded that infinite slope analysis is not appropriate for most deep landslides because "there are more differences, structurally and geometrically, between one deep-seated landslide and another than between shallow landslides." Furthermore, Baum and others (2008, p. 7) stated "deep-seated landslides tend to be less related to a single triggering event or group of events than populations of shallow landslides." Therefore for the protocol described here we have developed a different method to evaluate deep landslide susceptibility.

Although the methods we use are thorough and well tested, it is worth mentioning some limitations. One such limitation is that while researchers have recently developed a method to model displacement, velocity, and runout of large deep landslides (Iverson and others, 2015) and this model was successfully used to assist in emergency response and recovery at the 2014 Oso landslide, accurate displacement and runout GIS-based modeling is not within the current capabilities of deep-landslide modeling methods (Baum and others, 2008). Such a model is likely years away from becoming available for use on projects for regional mapping. Therefore, prediction or estimation of displacement or runout of deep landslides is not included in the method presented in this paper. Other limitations are described in section **6.0**.

The objective of this paper is to provide a protocol for developing, at an accelerated rate, consistent deep landslide susceptibility maps that identify areas with low, moderate, or high potential for deep landslides. The protocol is for internal use at DOGAMI as well as for the larger scientific community. By following this protocol, users can produce standardized maps more quickly and consistently. These maps can improve community awareness of deep landslide hazards, which will help the communities with landslide risk reduction activities.

The intended audiences for this paper include those in government, industry, and academia who are interested in producing standardized deep landslide hazard maps, and others who are interested in understanding how DOGAMI deep landslide susceptibility maps are made.

2.1   Definition of Deep Landslides

The term *landslide* includes a wide range of gravity-driven downslope movements of material that all have different types of movement, rates of movement, sizes, frequencies of movements, and triggering conditions, which result in different hazards. Major types of landslides are falls, topples, slides, spreads, and flows, as illustrated in **Figure 2.3**. Landslides in Oregon encompass all major movement types, and all these types are differentiated in landslide inventories created using in DOGAMI SP-42.

Figure 2.3.   Block diagrams and descriptions of some of the most common types of landslides (Burns and Madin, 2009a; modified from Highland, 2004; Varnes, 1978).

Falls are near-vertical, rapid movements of masses of materials, such as rocks or boulders. The rock debris sometimes accumulates as talus at the base of a cliff.

Topples are distinguished by forward rotation about some pivotal point, below or low in the mass.

Slides are downslope movement of soil or rock on a surface of rupture (failure plane or shear-zone).
- **Rotational** slides move along a surface of rupture that is curved and concave.
- **Translational** slides displace along a planar or undulating surface of rupture, sliding out over the original ground surface.

Spreads are commonly triggered by earthquakes, which can cause liquefaction of an underlying layer and extension and subsidence of commonly cohesive materials overlying liquefied layers.

Channelized Debris Flows commonly start on a steep, concave slope as a small slide or earth flow into a channel. As this mixture of landslide debris and water flows down the channel, it picks up more debris, water, and speed, and deposits in a fan at the outlet of the channel.

Earth Flows commonly have a characteristic "hourglass" shape. The slope material liquefies and runs out, forming a bowl or depression at the head.

Complex landslides are combinations of two or more types. A common complex landslide is a slump-earth flow, which usually exhibit slump features in the upper region and earth flow features near the toe.

As the name implies, deep landslides involve movement of a relatively thick layer of material (**Figure 2.4**). Many generally large deep landslides exhibit common features as shown in **Figure 2.5**.

The landslide mapping protocol described in DOGAMI SP-42 classifies landslide polygons as either deep or shallow on the basis of estimated or actual depth of movement. Separating shallow and deep landslide polygons is necessary because the methods used to delineate shallow and deep landslide susceptibility differ. Unfortunately, there is no widely accepted depth boundary between shallow and deep slides. For SP-42, we selected 15 ft (4.6 m) as the boundary between shallow and deep slides on the basis of the combination of several factors and results from other studies, discussed in detail in DOGAMI SP-42. *Therefore, for the purposes of this protocol, landslides, regardless of movement type, that move on a surface (or in a zone) 15 ft (4.6 m) or more below the ground surface are considered to be deep landslides.*

Figure 2.4.   Block diagrams of shallow (left) and deep (right) landslides (Burns and Madin, 2009a).
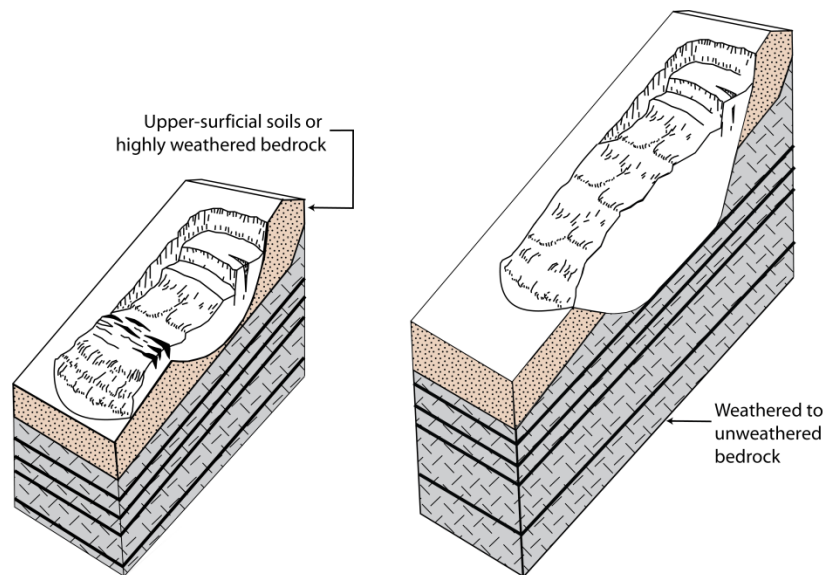
Figure 2.5.   Block diagram of a rotational earth slide-earth flow showing common features such as head scarp, flank, internal scarps, and toe (Burns and Madin, 2009a; modified from Highland, 2004; Varnes, 1978).
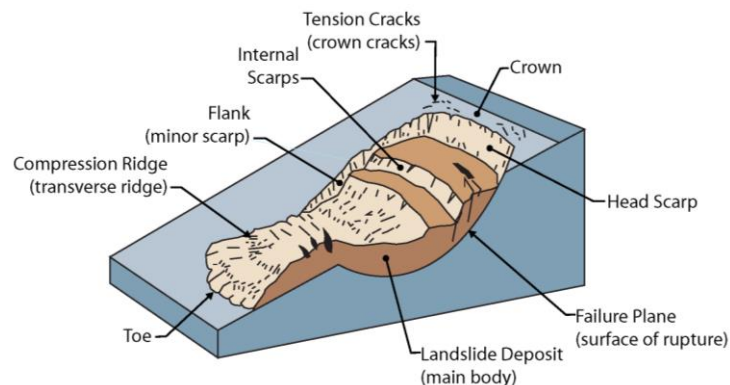
2.2   Discussion of Deep Landslides

Existing landslide deposits often remain in a weakened state. Many deposits tend to fail over and over. Three factors influence repeated failure: 1) material strength: the strength of the original geologic material generally decreases after landsliding has occurred; 2) permeability: the landslide material commonly increases in permeability, which results in an increase in rate of water infiltration and porosity to hold water; and 3) topography: the topography of the slide area can change significantly as moderate slopes change to steep slopes along the toe, internal scarps, and the head scarp. All three factors affect landslide susceptibility. Thus it is particularly important to identify previously failed areas (that is, existing landslides), as they may be at risk for future instability.

The current version of the Statewide Landslide Information Database for Oregon (SLIDO) 3.2 (Burns, 2014) contains a landslide inventory mapped by following the DOGAMI SP-42 protocol. SLIDO 3.2 classifies 8,490 landslides as deep. Of these, 2,639 are classified as historic (< 150 years old), and 5,851 are classified as prehistoric (> 150 years old) (Burns and Madin, 2009a). One quarter (621; 24%) of the mapped historic deep landslides intersect spatially with mapped prehistoric landslides. This number indicates that many younger (historic) landslides are most likely reactivated prehistoric landslides. More than half (5,134; 58%) of the deep landslides intersect spatially with other deep landslides. This is another indication that many deep landslides either are reactivations of portions of existing deep landslides or that they tend to cluster directly adjacent to each other. These findings suggest that the most likely locations for future deep landslides (deep landslide susceptibility) are within an existing deep landslide (reactivation) or directly adjacent to an existing deep landslide. This relationship underscores the importance of having a deep landslide inventory as a fundamental dataset when trying to predict future deep landslide susceptibility.

3.0 METHODOLOGY

3.1 Overview

The method we use to identify areas susceptible to deep landslides combines several datasets, many of which derive from deep landslide data extracted from an inventory created by following the DOGAMI SP-42 method (Burns and Madin, 2009a). We process each dataset and then combine the datasets into a final deep landslide susceptibility dataset of polygons that define areas of low, moderate, and high susceptibility to deep landslides. We accomplish all steps by using Esri® ArcMap® Geographic Information Systems (GIS) software. We describe each GIS process in the appendix; the general approach is presented below.

We selected Low, Moderate, and High as our zone classification scheme because these classes are consistent with the three zones in our shallow landslide susceptibility protocol (Burns and others, 2012a) and because dividing susceptibility into more zones would require finer-detail input data sets than we currently have available. The contributing datasets for each susceptibility zone are:

- 🔴 High susceptibility zone
  - o Inventory: landslide deposit polygons
  - o Inventory: head scarp-flank polygons
  - o Head scarp-flank polygon buffers
- 🟠 Moderate susceptibility zone
  - o Minimal moderate zone
  - o Combination of four factors
    - ▪ Susceptible geologic units
    - ▪ Susceptible geologic contacts
    - ▪ Susceptible slopes in each engineering geologic unit polygon
    - ▪ Preferred directions in each engineering geologic unit polygon
- ⚪ Low susceptibility zone
  - o Areas not identified in the high or moderate zones

To aid readers in understanding the sequence of steps required to complete this protocol, we provide throughout this paper a small graphical progress bar before each step that corresponds to the diagram shown in **Figure 3.1**. Box fill and arrow (▾) in the small graphical progress bar will indicate progression.

Figure 3.1. Graphical representation of the deep landslide susceptibility protocol discussed in this paper.
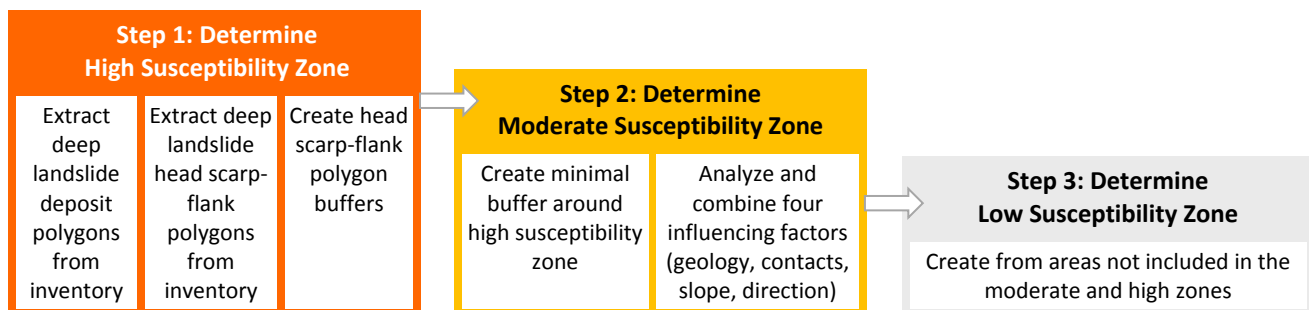
For ArcGIS file organization in this protocol, we use a standardized folder scheme to store working and final data. The folder names are:

- A_Landslide_Inventory
- B_Head_Scarp_Flank
- C_Geologic_Units
- D_Geologic_Contacts
- E_Slopes
- F_Directions
- G_Minimal_Moderate

To show the various components of the deep landslide susceptibility method in this paper, we use the northwestern quarter of the 7.5-minute U.S. Geological Survey (USGS) Oregon City quadrangle, for which we already had landslide inventory created using the protocol in SP-42 (**Figure 3.2;** Burns and Madin, 2009a, b).

Figure 3.2. Example of a lidar-based landslide inventory map for the northwest quarter of the 7.5 minute USGS Oregon City quadrangle (DOGAMI IMS-26, Burns and Madin, 2009b).
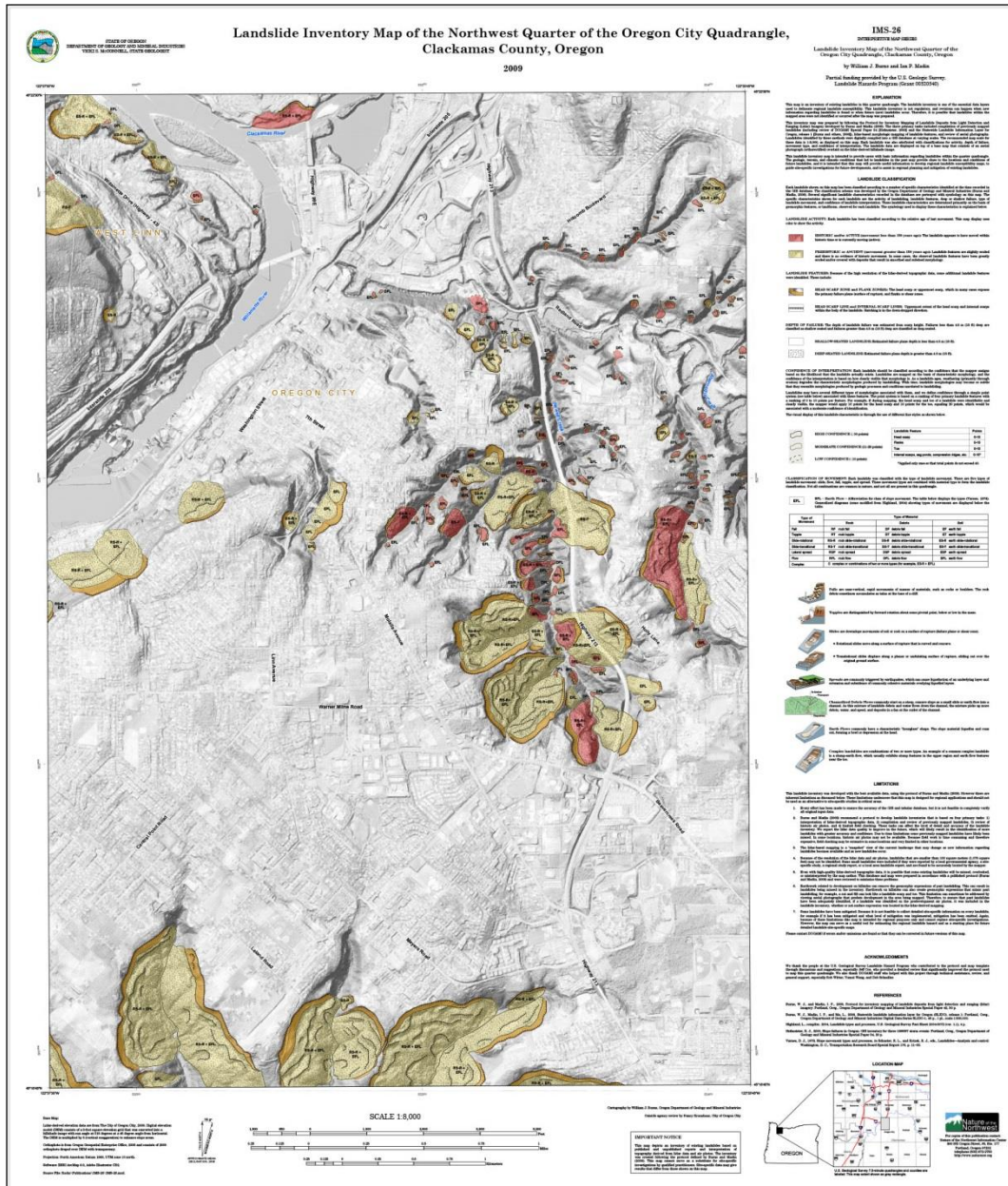
3.2   High Susceptibility Zone

A complete landslide inventory is needed to create the high susceptibility zone layer. This protocol assumes that an inventory has been created by following the landslide inventory protocol given in DOGAMI SP-42 (Burns and Madin, 2009a); such an inventory will look similar to the example shown in **Figure 3.2**.

Methodology progress bar: | **High Susceptibility** | ⇒ | **Moderate Susceptibility** | ⇒ | **Low Susceptibility** |

3.2.1   Deep Landslide Polygons

To obtain deep landslide polygons and their head scarp-flank polygons from the inventory we query the inventory database for deep landslide deposit polygons, then convert the polygons to a raster dataset with a cell size of 3 ft (0.91 m). Unless otherwise noted, all raster datasets in this method have a cell size of 3 ft (0.91 m), which is the cell size of the standard lidar-derived digital elevation models (DEM) for Oregon. **Figure 3.3** shows an example of the resulting raster dataset.

Figure 3.3.   Example of deep landslide deposits from a landslide inventory converted to a high susceptibility zone raster layer (red areas on map). The area shown corresponds to the Oregon City quarter quadrangle shown in Figure 3.2.

Methodology progress bar:	High Susceptibility ▼	⇨	Moderate Susceptibility	⇨	Low Susceptibility
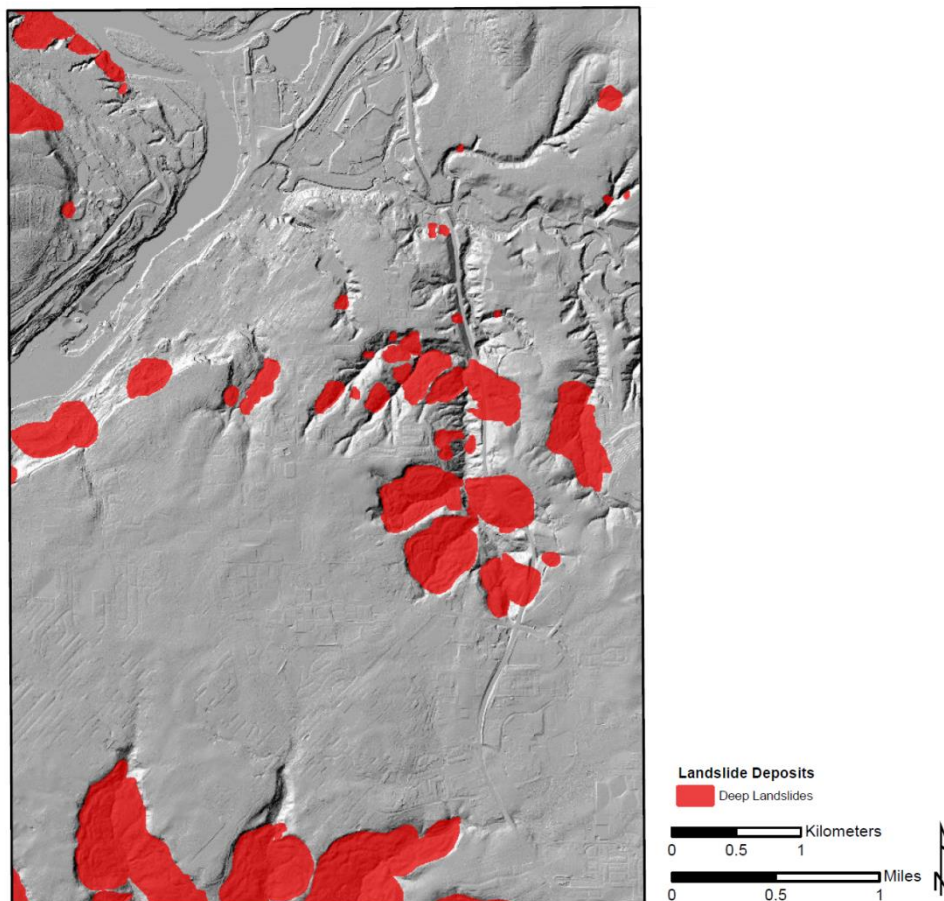
3.2.2   Head Scarp-Flank Polygons

All deep head scarp-flank polygons are queried out of the inventory database and saved as a shapefile (see appendix). The head scarp-flank polygons are considered areas of high susceptibility and are included as part of the head scarp-flank polygon buffers discussed next. Therefore they do not need to be converted to a raster image.

Methodology progress bar:	High Susceptibility ▼	⇨	Moderate Susceptibility	⇨	Low Susceptibility

3.2.3   Buffers

Most landslides tend to have a steep head scarp above the failed mass. The head scarp area will commonly fail retrogressively or a separate landslide will form above the head scarp because of the loss of resisting forces directly adjacent to and below the head scarp. To account for the increase in susceptibility of the area above head scarp, we apply a buffer around the head scarp-flank polygons.

Two buffers are created for each head scarp-flank polygon: 1) a head scarp-flank retrogression buffer, and 2) a 2:1 horizontal distance to vertical distance (2H:1V) buffer. For each head scarp-flank polygon the greater of the two buffer values is used for later calculations. Generally, the first buffer (head scarp retrogression) results in a larger buffer distance value. This is likely because in most landslides the horizontal distance (H) or average horizontal distance of the internal down-dropped blocks is generally more than the depth (V) (see upper down-dropped block and failure depth in **Figure 2.5**). Of the 8,490 deep landslides in the SLIDO 3.2 inventory, 1,178 have a recorded average internal down-dropped block horizontal distance. The mean of the average horizontal distances is 172 ft (52 m), and the mean of the failure depths is 53 ft (16 m). This indicates that, overall, horizontal distance is generally more than depth.

3.2.3.1   Head Scarp-Flank Polygon Retrogression Buffer

Many deep landslides move repeatedly over hundreds or thousands of years and, commonly, the continued movement is through retrogressive failure (continued upslope failure) of the head scarp into the crown (**Figure 2.5**). To account for this potential upslope hazard, we apply a buffer to all head scarp-flank polygons as shown in **Figure 3.4**. To determine the head scarp retrogression buffer, we calculate the average horizontal distance (as defined in **Figure 3.4**) of the internal down-dropped blocks (assumed to be previous retrogression failures). If the SP-42 protocol was used when creating an initial landslide inventory, the average horizontal distance has already been calculated. This average horizontal distance is different for each head scarp and is dependent on the horizontal distance between internal scarps. Some landslides do not have internal blocks. This is likely related to the type of process and/or the age of the landslides. For example,, some deep landslides are primarily earth flows, which commonly do not have internal blocks. Also, internal features can become obscured over time and may be unrecognizable and thus unmappable.

Figure 3.4.   Head scarp-flank retrogression buffer.
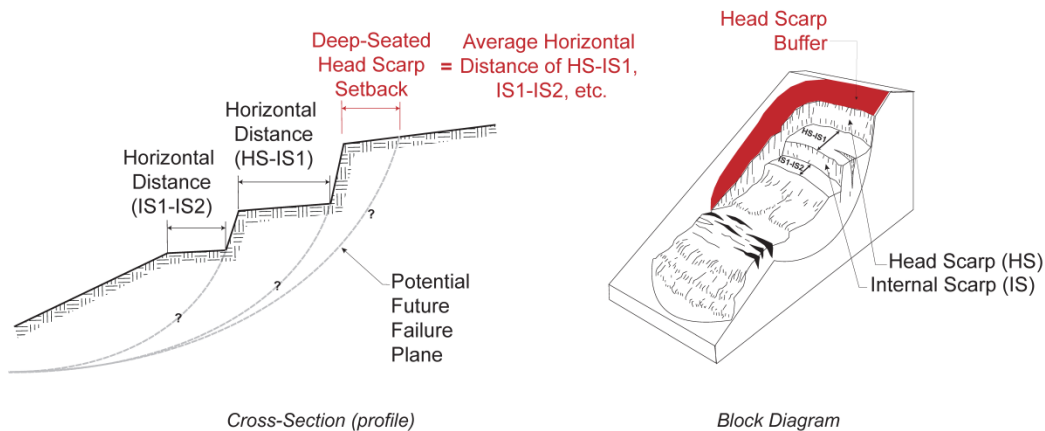
3.2.3.2 2H:1V Head Scarp-Flank Polygon Buffer

Most natural, unfailed (non-landslide) geologic materials have an angle of internal friction or equivalent shear strength of at least 26 degrees. Because the slope angle of 26 degrees is equal to the slope ratio of 2H:1V (see **Figure 3.5**[A]), geotechnical engineers commonly use 2H:1V as a proxy for slope stability. This ratio is also supported by SLIDO 3.2 landslide inventory data: generally, as previously noted, horizontal distances are more than depth distances.

To create the head scarp-flank polygon buffers, we add a field to the Head_ScarpFlanks shapefile (see appendix). In the new field, we enter twice the depth of failure of each individual landslide. This result is different for each head scarp. For example, a head scarp height of 25 ft has a 2H:1V buffer equal to 50 ft.

Figure 3.5.   Diagram of the 2H:1V head scarp buffer (orange on block diagram).
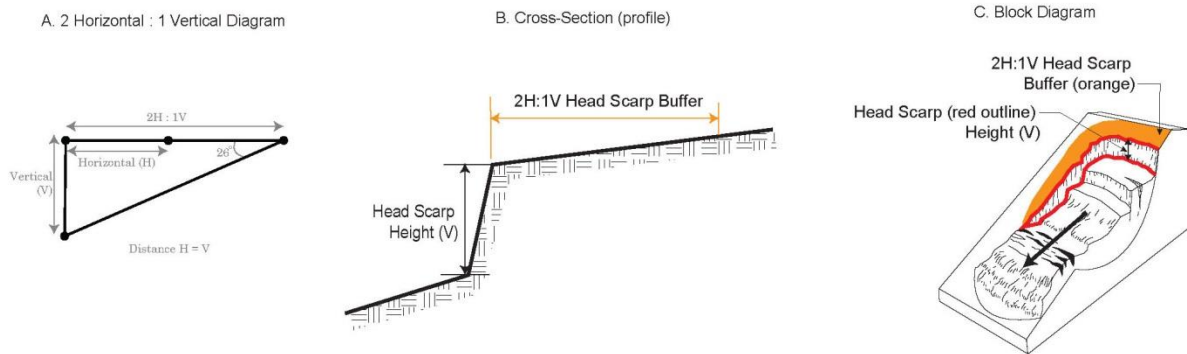
After we create the two buffer field values, we use the larger of the two values for each head scarp-flank polygon to make this part of the High susceptibility zone. **Figure 3.6** shows an example of a buffer map.

Figure 3.6. Example of the buffered deep landslide head scarp-flank polygons converted to high susceptibility zone (red areas on map). Darker red areas are the mapped head scarp-flank polygons. The area shown corresponds to the Oregon City quarter quadrangle shown in Figure 3.2.
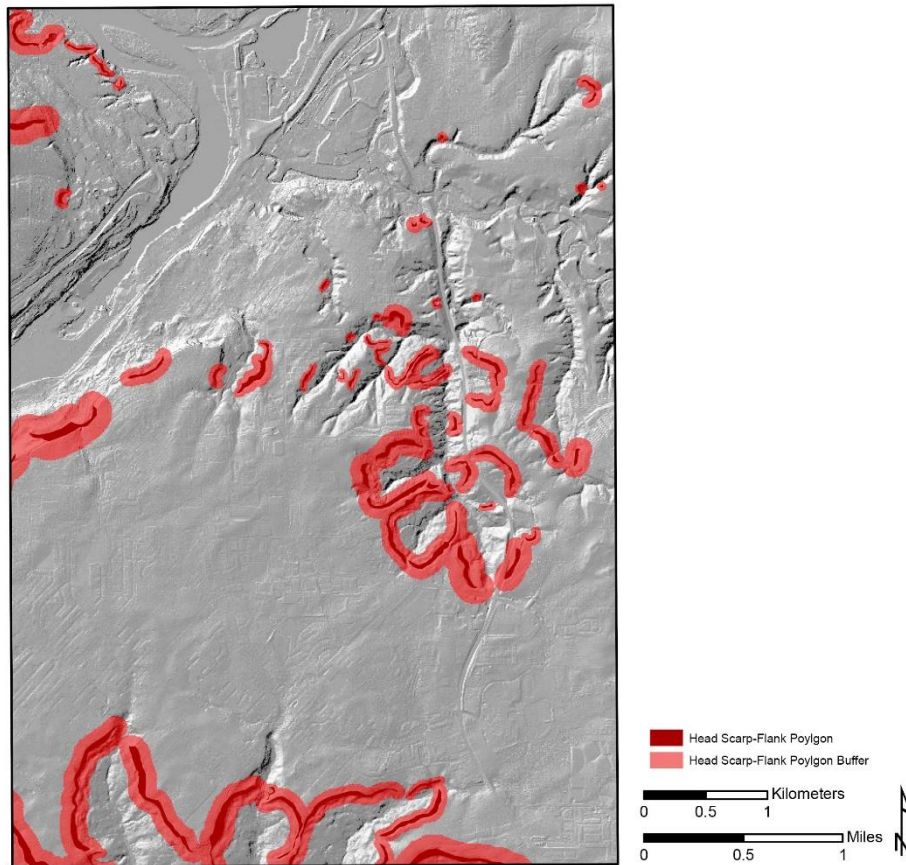
Finally, we combine the landslide deposits and buffered head scarp-flanks (see appendix) to create the final deep landslide high susceptibility zone layer:

Landslide deposits   plus   buffered head scarp-flanks   results in   final high susceptibility zone.
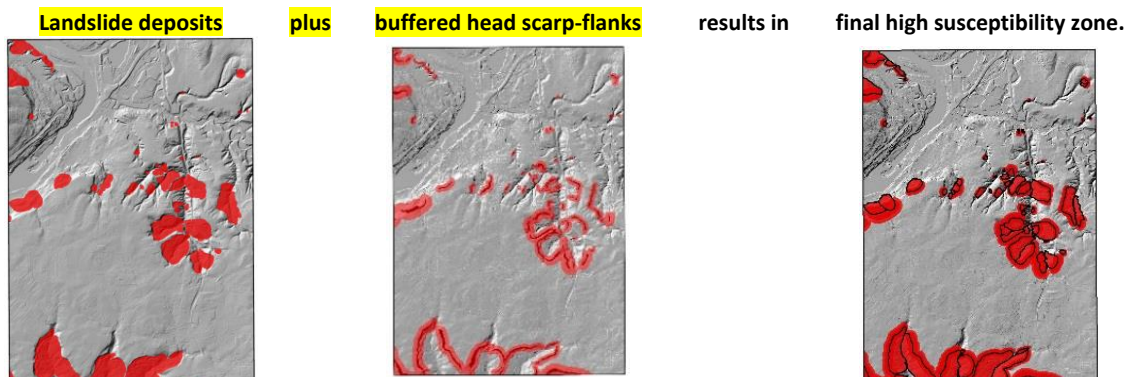
3.3   Moderate Susceptibility Zone

In order to ensure that the final susceptibility map does not spatially change directly from high to low without some transition, we recommend creating a moderate zone around all high zones. We create the moderate susceptibility zone by first adding a minimal moderate zone around the high susceptibility zone (section 3.3.1) and then expanding the zone by factoring in geologic criteria (section 3.3.2).

Methodology progress bar:

| High Susceptibility | ⇒ | Moderate Susceptibility ▼ | ⇒ | Low Susceptibility |
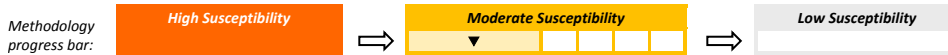
3.3.1   Minimal Moderate Susceptibility Zone Buffer

To establish a minimal buffer around the deep landslide deposits and the head scarp-flank polygons (together composing the high susceptibility zone), we multiply the head-scarp height by 2. This establishes a minimal distance that varies for each landslide on the basis of the landslide's attributes (**Figure 3.7**). Some landslide deposits do not have a mappable head scarp-flank polygon and thus may not have a head scarp height. In these cases, we use the minimum head scarp height, which is 15 ft (recall that we selected 15 ft [4.6 m] as the boundary between shallow and deep slides); this results in a minimum minimal moderate buffer of 30 ft.

Figure 3.7.   Map of the high susceptibility zone (red) and the minimal moderate susceptibility zone (orange). The area shown corresponds to the Oregon City quarter quadrangle shown in Figure 3.2.

Methodology progress bar:	High Susceptibility	⇒	Moderate Susceptibility ▼ ☐ ☐ ☐ ☐	⇒	Low Susceptibility
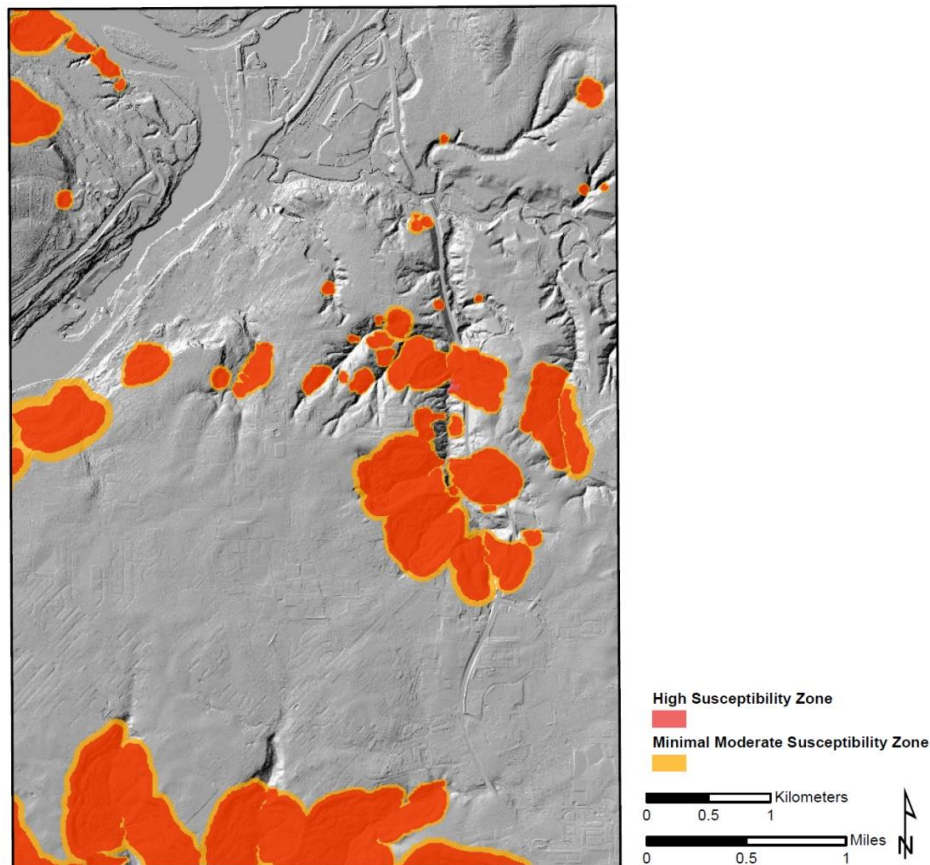
3.3.2 Moderate Zone Influencing Factors Score Layer

We expand the minimal buffer by examining geologic factors. The four factors used to establish the combined moderate factors score layer are:

- Susceptible geologic units
- Susceptible geologic contacts
- Susceptible slope angles for each engineering geologic unit polygon
- Preferred direction of movement

The combined moderate factors score layer is the result of a qualitative method also known as a weighted parameter regional landslide hazard analysis (Baum and others, 2008). The main advantage of this type of analysis is that it is relatively rapid and most of the data needed for the method are commonly available or are easily acquired or calculated. The main disadvantage is that the method depends on the investigator's judgment and thus is subjective and may be hard to replicate by others (Baum and others, 2008). Other methods exist to evaluate deep landslide susceptibility. Baum and others (2008) discussed the advantages and disadvantages of many of these methods. Some of these methods result in objective, statistical, and/or probabilistic output maps, but the input data can take much more time to collect and thus can lead to higher costs and longer map production times. Because our objective is to create deep landslide susceptibility maps for large areas of Oregon (cities and counties) at an accelerated rate, the combined moderate factors score layer qualitative method is suitable.

We selected the factors on the basis of reasons described in each factor's respective subsection below. Some factors have been used by or are recommended by others to predict future deep landslide susceptibility. For example, Giraud and Shaw (2007) used geologic and slope maps to create a landslide susceptibility map of Utah; Soeters and van Westen (1996) and Sidle and Ochiai (2006) concluded that geomorphology (landslide inventory), topography, engineering geology, land use, vegetation, and hydrology should be used as the primary input data for regional large-scale mapping. Because some of these factors can change rapidly over time and are much better suited for shallow landslide susceptibility analysis, we selected only a subset of these factors. For example, we chose not to include forest cover (vegetation). Forest cover can change from a mature forest to a clear cut in less than a year. The presence of trees influences near-surface soils (by root strength and by the rate which rainfall reaches the ground surface and infiltrates near-surface soils) and so affects shallow landslide stability, but forest cover affects deep landslide stability much less.

Another data set sometimes considered in landslide susceptibility mapping is distance to faults. However, because not all landslides are triggered by faults and our susceptibility method is non-trigger specific, we chose not to include the fault dataset. As further support of our choice, Safran and others (2011, p. 1) in a recent study of large landslides in Oregon stated "fault density exerts no control on landslide distribution."

3.3.2.1 Bedrock Engineering Geologic Map

For deep landslide susceptibility, we use four factors partially derived from a bedrock engineering geologic map. Generally, the mapper will need to create the bedrock engineering geologic map. Engineering geology maps are generally based on geotechnical properties and engineering behavior derived from a standard lithostratigraphical geologic map (Dobbs and others, 2012). Such maps are commonly divided into bedrock engineering geologic and surficial engineering geology (Keaton and Degraff, 1996).

   The first task in creating a bedrock engineering geologic map is to remove any landslide polygons from the standard lithostratigraphical geologic map. For most cases, each landslide polygon is simply merged with the surrounding bedrock geologic unit. If a landslide polygon crosses bedrock units, the polygon is divided into two or more polygons; each landslide polygon is then merged with the surrounding unit (**Figure 3.8**). In rare cases, such as in project areas spanning multiple counties or larger regions, the semi-automated methods described by Burns and others (2015) can be used for this task.

Figure 3.8.   Geologic bedrock map with landslides polygons removed (Ma and others, 2009). The area shown corresponds to the Oregon City quarter quadrangle shown in Figure 3.2.
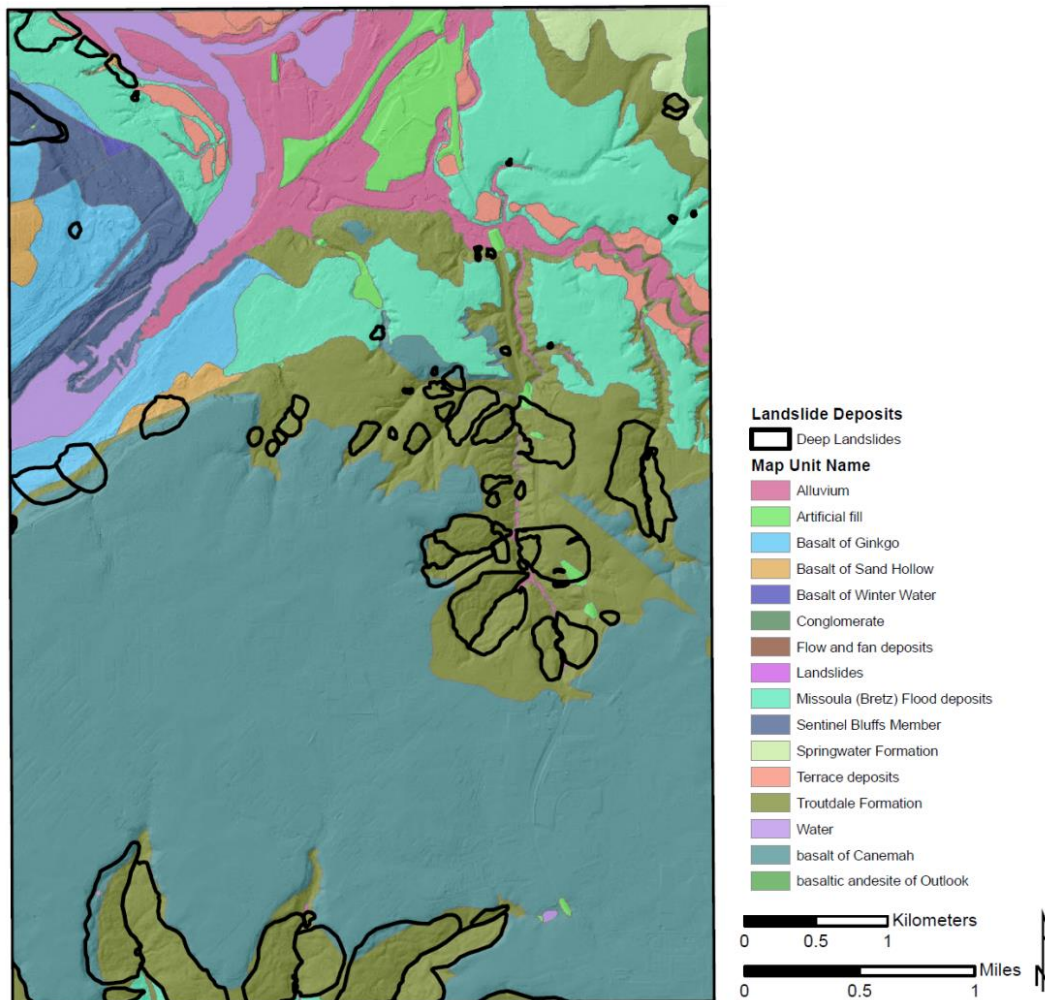
After removing landslide polygons, combine the geologic map units into bedrock engineering geologic map unit properties. To do this, we start by examining the general spatial correlation between the landslides and the geologic units and contacts. This is because the four moderate susceptibility score factors are based on statistics between the bedrock engineering geologic units and the landslides within those units.

Once we have a general spatial correlation between geologic units and the landslides, we convert the geologic map to the bedrock engineering geologic map. We start by removing any water polygons and thin alluvium polygons along the water polygons. Alternatively, if these polygons do not cover a large spatial extent, we merge them with the surrounding bedrock (Figure 3.8; water and alluvium). In addition, unless artificial fill (**Figure 3.8**) is relatively thick and contains deep landslides, we merge these polygons with the surrounding geology polygons.

Next, we add an engineering geologic unit field to the bedrock engineering geologic map. We classify each geologic unit from the original geologic map with a new engineering geologic map unit based on attributes similar to those shown in **Table 3-1**. This classification scheme is derived from those of Dobbs and others (2012) and Keaton and Degraff (1996, Unified Rock Classification System).

Table 3-1.   Bedrock engineering geologic map unit classification scheme.

Attributes *					Example Engineering Geology Unit Based on Attributes
Genetic Origin	Strength	Mechanics / Chemistry	Grain Size, Texture	Degree of Weathering	
Sedimentary	soft loose stiff dense weak medium strong strong very strong	soil rock bedded massive carbonate or noncarbonate	fine-grained mixed-grained coarse-grained limestone dolomite mudstone sandstone conglomerate	none slight moderate severe complete	Weak Mudstone
Metamorphic	weak medium strong strong	foliated bedded massive	slate schist gneiss marble serpentinite fine medium coarse	none slight moderate severe complete	Fine Medium Strong Slate
Igneous	weak medium strong strong	intrusive extrusive	granite andesite basalt rhyolite volcaniclastic tuff	none slight moderate severe complete	Weak Severely Weathered Volcaniclastic

Classification scheme modified from Dobbs and others (2012) and Keaton and Degraff (1996).

It is important to note that although in creating our geologic engineering map we make use of the modified classification of Dobbs and others (2012) and Keaton and Degraff (1996), our final engineering map differs from most standard geologic engineering maps. In areas where landslides cross geologic unit contacts, we keep separate some very similar geologic units that would normally be combined into a single engineering geologic unit. **Figure 3.8** shows an example of this departure from the standard classification scheme; here, we did not combine two very similar basalt units (Ginkgo and Winter Water, both members of the Columbia River Basalt Group) in the northwest corner of the map because a landslide crosses the contact.

Figure 3.9 shows an example of an engineering geology map created using our method, in which similar geologic units have not been combined into a bedrock engineering geologic unit because landslide cross them.

Figure 3.9.   Engineering geology map. The area shown corresponds to the Oregon City quarter quadrangle shown in Figure 3.2.

| High Susceptibility | | Moderate Susceptibility | | Low Susceptibility |
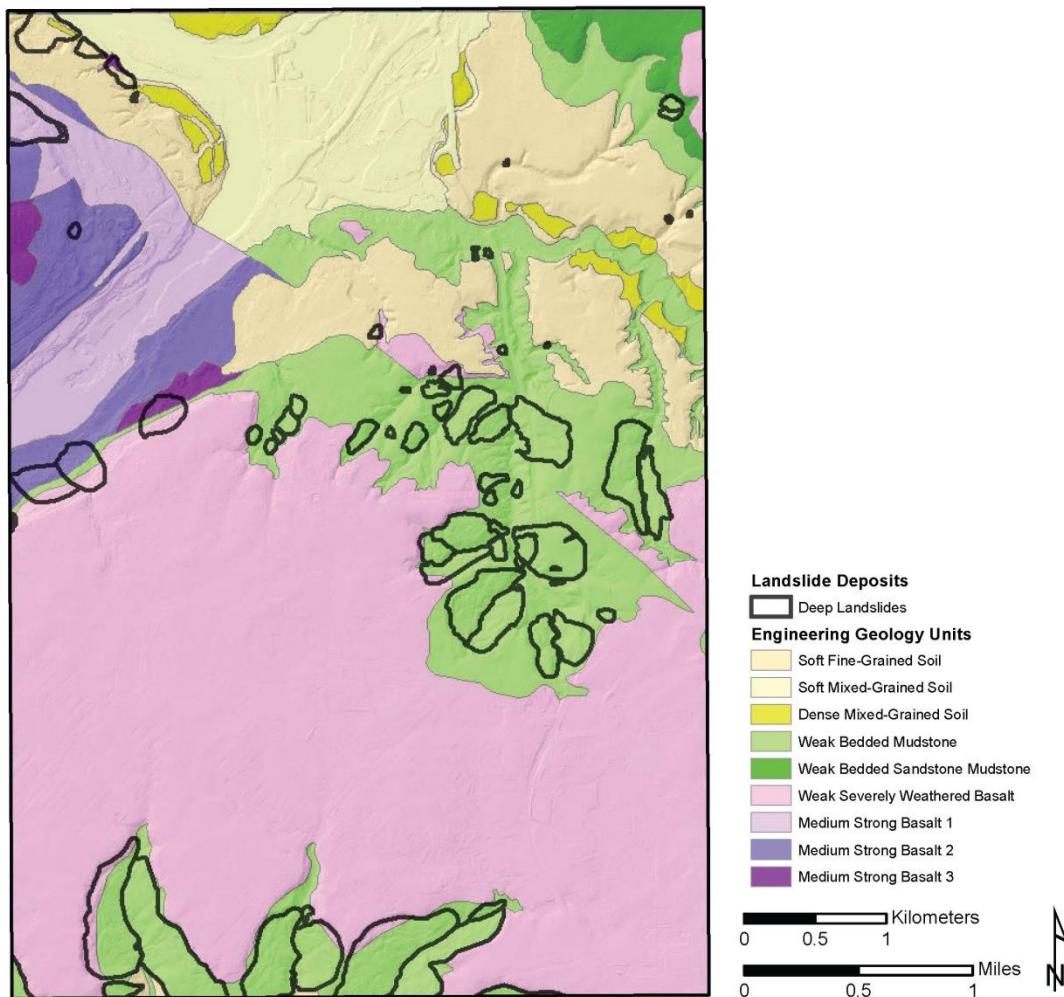
3.3.2.2 Factor Maps

3.3.2.2.1 Susceptible Geologic Units

Once we have a bedrock engineering geologic map, we can begin to create the four individual factor maps. The first factor, susceptible geologic units, has a relatively widespread correlation with surficial processes. For example, it is very common that certain geologic formations or units are more or less prone to landslides. This is generally due to the properties of the rock such as material strength or bedding planes.

To determine how susceptible each engineering geologic unit is to deep landslides, we calculate the ratio of total area of landslides within each unit to that unit's total area. We call this ratio the landslide density. We prefer calculating landslide density to simply counting landslides per unit because deep landslides can be very large and counting by unit can dramatically underestimate the susceptibility of the unit. We use landslide density class thresholds developed by Burns and others (2015). Burns and others created a statewide landslide susceptibility overview map of Oregon by calculating landslide density and determining minimum, maximum, mean, and standard deviation for generalized engineering geologic units. They intersected 148 generalized geologic units with landslide inventory polygons from SLIDO 3.2 (Burns, 2014); 119 of the 148 units contained landslides. Landslide density ranged from ~0% to just over 45% (**Figure 3.10**). They selected 7% and 17% as thresholds for landslide density relative hazard classes:

- High landslide density – greater than 17%
- Moderate landslide density – 7% to 17%
- Low landslide density – less than 7%

Figure 3.10. Histogram of landslide density per generalized geologic unit for the statewide landslide susceptibility overview map of Oregon (Burns and others, 2015). Of the 148 generalized geologic units, 119 contained landslides. Thresholds of 7% and 17% were chosen to separate landslide density relative hazard classes.
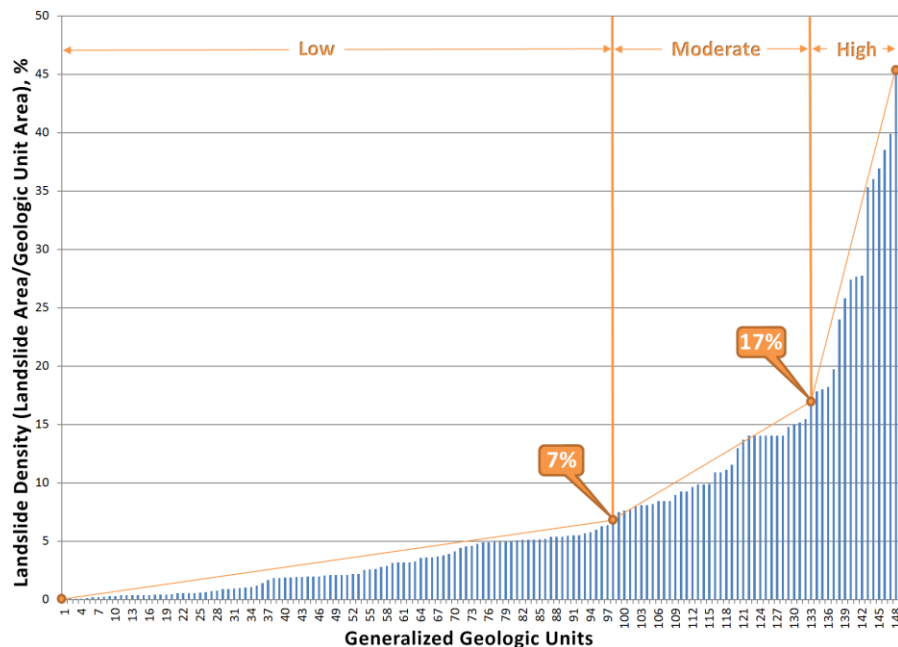
The thresholds selected in the statewide survey are somewhat similar to landslide incidence thresholds (>15% [high], 1.5%–15% [medium], and <1.5% [low]) established by the U.S. Geologic Survey for a landslide overview map of the conterminous United States (Radbruch-Hall and others, 1982).

The statewide landslide density thresholds also define categories that are comparable to high and moderate landslide hazard classes in other studies where classes were determined by using different methods (**Table 3-2**), so we are confident in using these same thresholds for our deep landslide susceptibility mapping protocol.

Table 3-2. Other landslide inventories, percent coverage, and determined landslide hazard in Oregon.

Project	Percent Landslide Inventory Deposits	Landslide Hazard
Astoria (Burns and others, 2013)	27%	high
North Fork Siuslaw Watershed (Burns and others 2012b)	37%	high
Curry County (Burns and others, 2014)	25%	high
Bull Run Watershed (Burns and others, 2015)	15%	moderate to high

For the protocol, to create a map that shows susceptible geologic units we calculate landslide density for each engineering geologic unit, then apply our thresholds to assign a score of 0, 1, or 2 to each engineering geologic unit:

- Score = 0, if less 7% landslide density
- Score = 1, if less than 17% and greater than or equal to 7% landslide density
- Score = 2, if equal or greater than 17% landslide density

Therefore, in our example map (**Figure 3.9**), Weak Bedded Mudstone has a susceptible geologic unit score of 2; Medium Strong Basalt 3 unit has a score of 1; and the other units have a score of 0 (**Figure 3.11**). **Figure 3.12** shows a map of the resulting susceptible geologic unit scores.

Figure 3.11. Susceptible geologic unit (landslide density) scores for the area shown in Figure 3.9.
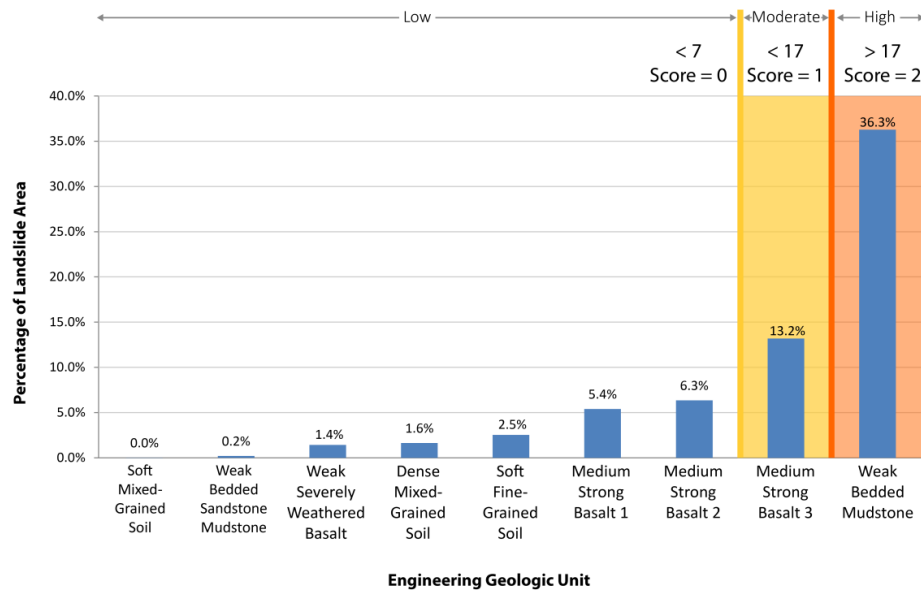
Figure 3.12. Map showing susceptible geologic units with scores of 0 (no color), 1 (orange), and 2 (red). The area shown corresponds to the Oregon City quarter quadrangle shown in Figure 3.2.
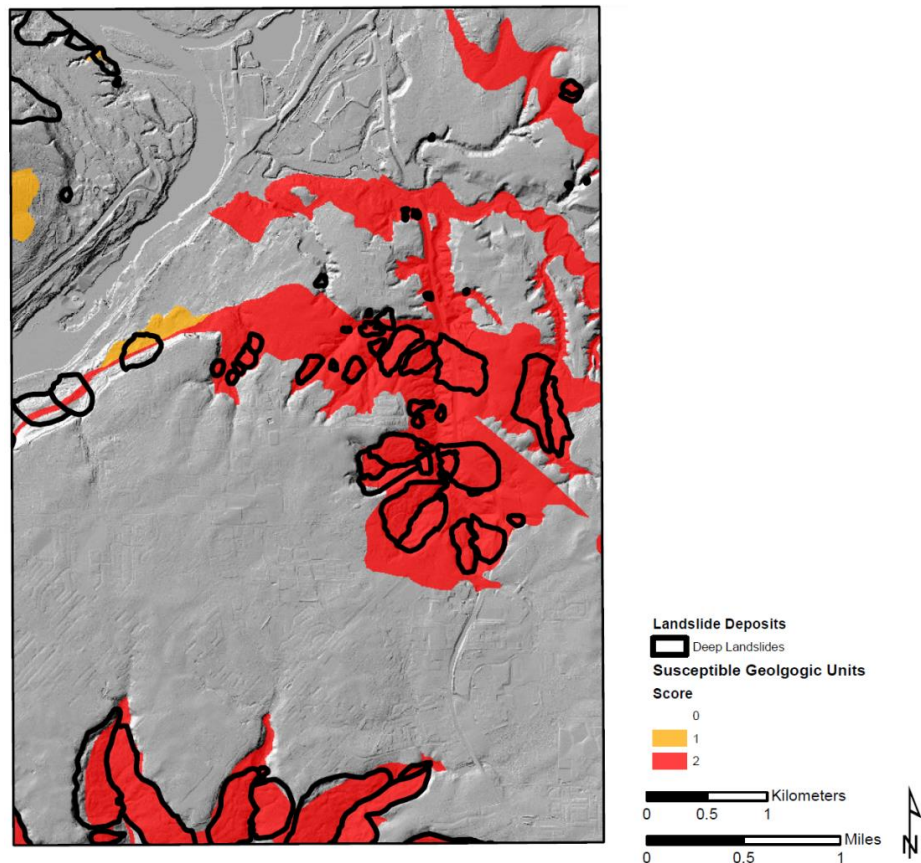
Because the deep landslide susceptibility method used here is for maps at a much larger scale (1:8,000)—and therefore the number of engineering geologic unit polygons and the contact complexity is greater—than at the 1:500,000 scale statewide scale, at this step in the protocol there may be cases where a mapper needs to use judgment to override the default calculated susceptible geologic unit score. In our example, Soft Fine-Grained Soil (2.5%), Medium Strong Basalt 1 (5.4%), and Medium Strong Basalt 2 (6.3%) all have percentages less than the statewide established 7%. However, in this local area, all three of these units have deep landslides associated with them (**Figure 3.9**). Therefore we manually change the score of 0 to a score of 1 for these three units. Additional studies at detailed scales may determine that lowering the threshold for such maps rather than manually adjusting scores is more efficient. **Figure 3.13** displays the final susceptible geologic units score map.

Figure 3.13. Map showing the final susceptible geologic unit factors with scores ranging from zero (no color), one (orange), and two (red). The area shown corresponds to the Oregon City quarter quadrangle shown in Figure 3.2.

Methodology
progress bar:

| High Susceptibility | | Moderate Susceptibility | | Low Susceptibility |
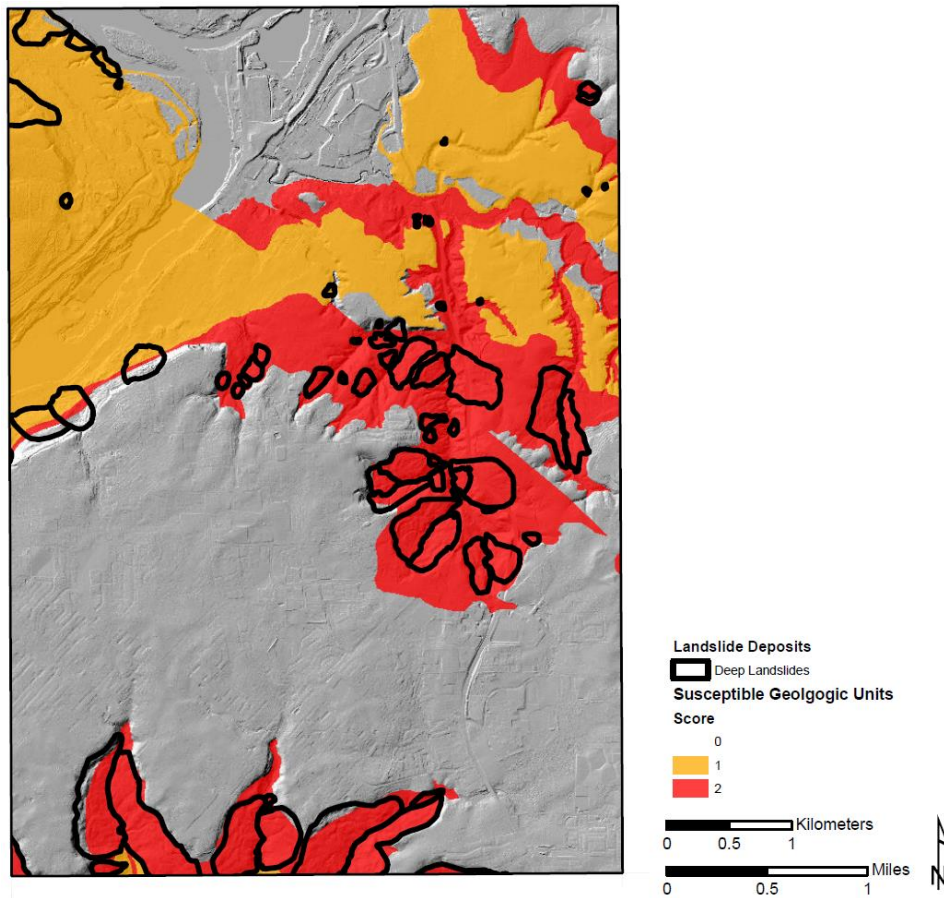
3.3.2.2.2 Susceptible Geologic Contacts

The second factor, susceptible geologic contacts, is the spatial overlap between landslides and geologic contacts. With the advent of lidar-based mapping in Oregon we and others (Safran and others, 2011) have begun to observe this relationship. Safran and others (2011, p. 1) stated "[l]andslides predominantly occur where even modest local relief (~100 m) exists near key contacts between weak sedimentary or volcaniclastic rock and coherent cap rock." We also have noticed that many landslides occur along a contact, especially when a sedimentary or volcanoclastic unit is overlain by an igneous unit (cap rock). Commonly, as streams and rivers cut down, they create relief and expose the underlying weaker unit. Once enough of the underlying weaker unit is exposed, the landslide process begins. Commonly, the landslide debris itself then erodes, and downcutting continues. For example, in the Oregon City area, large deep landslides are located next to each other along the contact between the basalt of Canemah (Boring Lava) and the underlying Troutdale Formation (**Figure 3.8**). Most of the landslide failure surfaces are almost completely within the Troutdale Formation, so they are not failing or sliding along the "geologic contact" in the sense that the failure plane follows the contact below ground. Rather, it is a spatial relationship between the landslides and the geologic unit contact surface traces (the contact lines on a map).

The first step defining susceptible geologic contracts is to identify contacts in the study area that have landslides along them. We use the following criteria:

Case 1:

The landslide deposit and/or head scarp-flank polygon is completely in the study area and

- intersects the contact, or
- is within a couple hundred feet (60 m) of the contact)

Case 2:

The landslide deposit and/or head scarp-flank polygon intersects a known landslide just outside the study extent and

- intersects the contact, or
- is within a couple hundred feet of the contact or is known to be associated with that contact.

For example, there are many landslides along the contact between Weak Bedded Mudstone and Weak Severely Weathered Basalt (**Figure 3.9** and **Figure 3.14**), so the contact and all the landslides and head scarp-flank polygons meet the criteria.

Figure 3.14. **Example of a susceptible geologic contact. This figure shows the intersection of landslide deposits (black lines) and their head scarp-flank polygons (red lines) with the contact between Weak Bedded Mudstone (green area) and Weak Severely Weathered Basalt (pink area).**
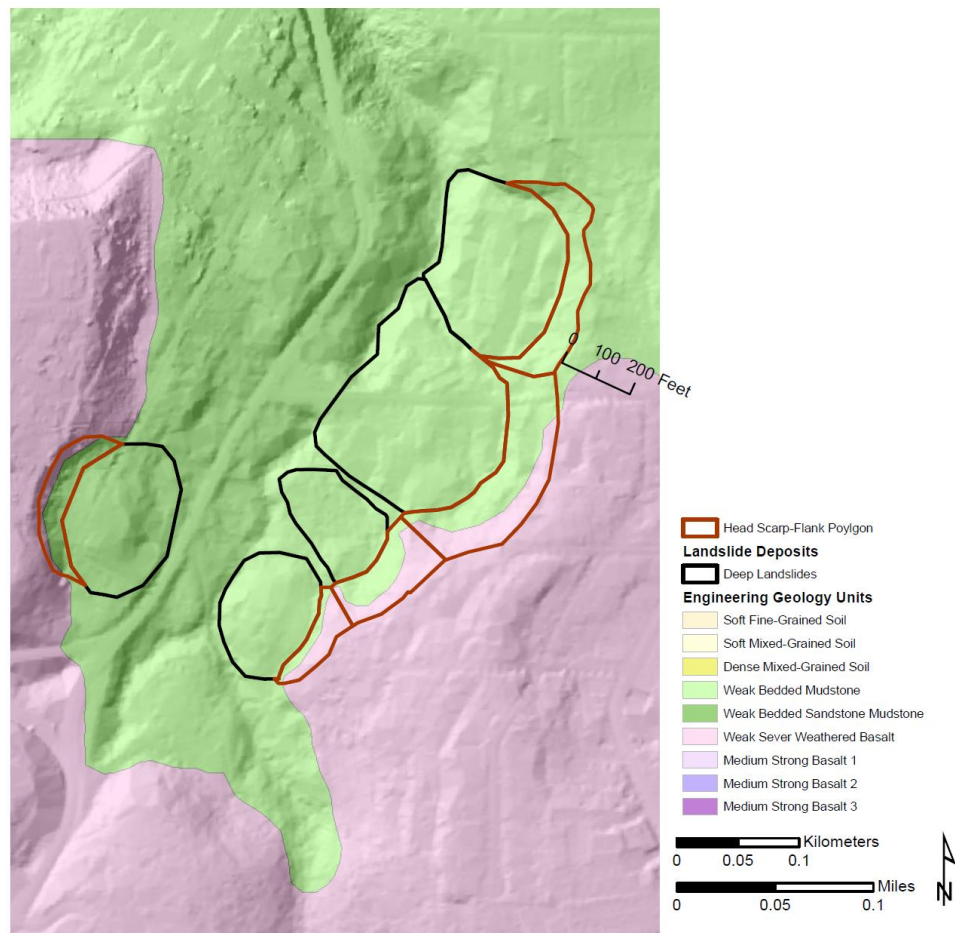
Once we have identified a susceptible geologic contact, we select the engineering geologic unit polygons on both sides of the contact and convert the polygons to lines (see appendix). We use a line symbol with a hash mark on the topological right side of the contact line to keep track of right and left sides of the lines (red line with hash marks in **Figure 3.15**). Then, we visually inspect the area on the topological right side of the contact to determine the location of the average distance from the contact to the head or toe of the landslide and use the measurement tool to find the distance value. (**Figure 3.15**). We repeat this process for the topological left side of the contact. We collect the right and left side measurements in a spreadsheet and calculate the mean and maximum for the right and left distance for all landslides for each contact line.

Figure 3.15. Example distance measurements on the right and left sides of the contact. The red line is the selected contact and the hash marks are on the topographically right of the contact.
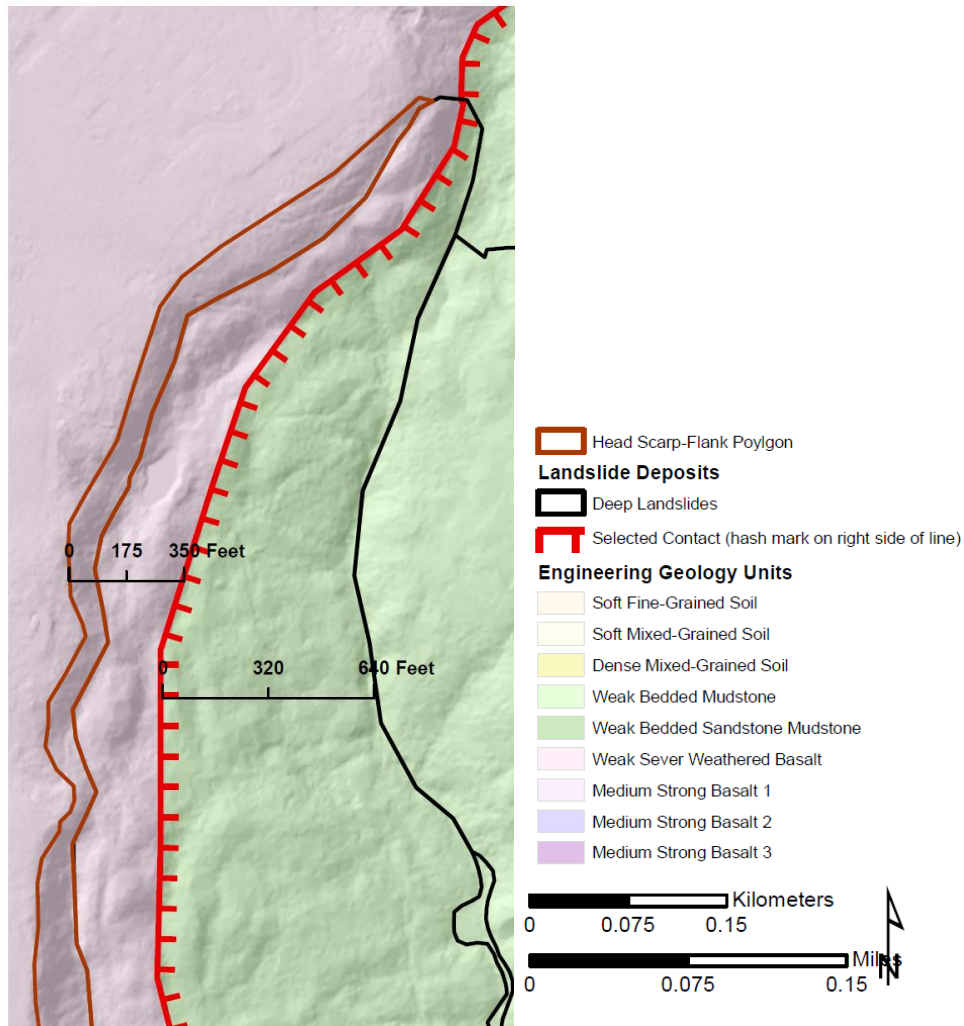
Next, we enter the mean and maximum for each contact as attributes in the contact line file. Then we buffer each line on the right and left with the mean and maximum, which results in four buffers. We combine the two mean buffers (right and left) and give the result a susceptible geologic contact score of 2; we combine the two maximum buffers (right and left) and give the result a susceptible geologic contact score of 1. Area outside these buffers is assigned a score of 0. We use the mean and maximum distances so that all distances above and below the contacts are captured. The mean distance gets the higher score (2), while the maximum distance gets the moderate score (1). The final susceptible geologic contacts scores map looks similar to **Figure 3.16**. In cases where there is only one landslide deposit along a contact, the mean and maximum distances are equal. This results in a single buffer around these contacts with a score of 2 (as shown in the northwest portion of **Figure 3.16**).

Figure 3.16. Map showing susceptible geologic contact scores of 0 (no color, gray), 1 (orange), and 2 (red). The contacts are the yellow lines, and the landslide deposits are outlined in black. The area shown corresponds to the Oregon City quarter quadrangle shown in Figure 3.2.
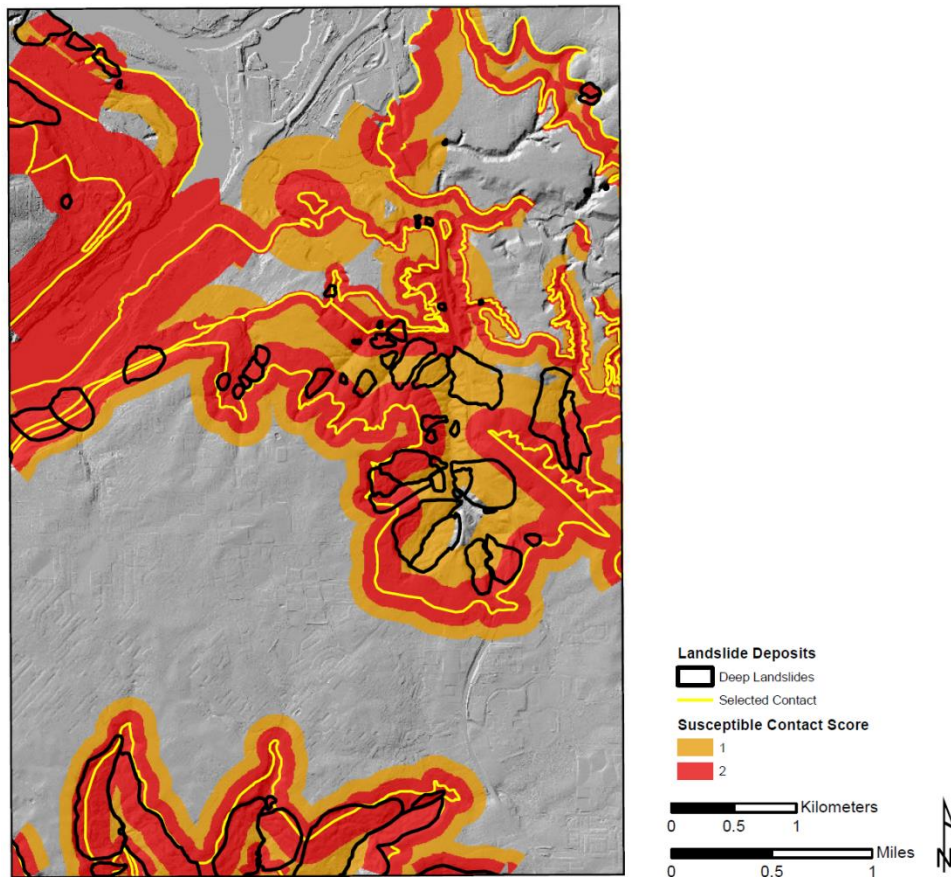
3.3.2.2.3 Susceptible Slopes

The third factor, susceptible slope angles for each engineering geologic unit polygon, generally correlates with landslide susceptibility. Most landslide susceptibility maps use slope as the primary factor or as at least one of the factors to predict future landslide locations. It is very common to see shallow landslides associated with steeper slopes. Deep landslides, on the other hand, appear to have less correlation with slope steepness, which is one reason we include the other three factors (geologic unit, contact, and direction).

Recall that inventories created by using the SP-42 protocol contain an estimate for pre-failure slope angles. We use these inventory data to calculate statistics for the pre-failure slope angles within each engineering geologic unit. We then use the statistics to determine the slope threshold values to divide slopes into a high, moderate, or low susceptibility slope score classes.

We use relief to reduce the areal extent of the slope factor, because inaccurate results can occur when slope alone is examined. The bare-earth lidar DEMs available for Oregon typically have a raster cell size of 3 ft^2 (1 m^2). When DEMs with such high resolution are converted to a slope map, some areas are falsely classified as having moderate or high deep landslide susceptible slopes. This occurs because many fine-scale topographic features like ditches, small retaining walls, and road cuts, common in developed landscapes, are represented in the lidar DEMs but do not have sufficient vertical or lateral extent to pose a significant deep landslide hazard.

Burns and others (2012a) concluded that focal statistics (a type of neighborhood analysis) was the best method to remove areas of very low relief from the shallow landslide susceptibility model. We use the same focal statistics method here to remove low to moderate relief from the deep landslide susceptibility model, with one revision.

The shallow landslide susceptibility model uses a neighborhood size of 15 ft^2 and a vertical relief of 15 ft. However, for deep landslide susceptibility, we use a neighborhood value of 100 ft^2. We chose this value by examining the data in SLIDO 4.0 (Burns, in press). This inventory has 9,126 deep landslides. Ninety-five percent of deep landslides are larger than 10,000 ft^2 (929 m^2). If we assume most deep landslides have relatively similar lengths and widths, we have, in effect, a square (or GIS neighborhood) of 100 ft^2. We take this to be a reasonable *minimum* area for deep landslides. Thus, area with less than 15 ft (4.5 m) relief across the 100-ft^2 neighborhood are removed from the final susceptible slopes score map (**Figure 3.17**).

Figure 3.17. Map of areas with less than 15 ft (4.5 m) of relief (purple area) over the 100-ft² neighborhoods. The area shown corresponds to the Oregon City quarter quadrangle shown in Figure 3.2.
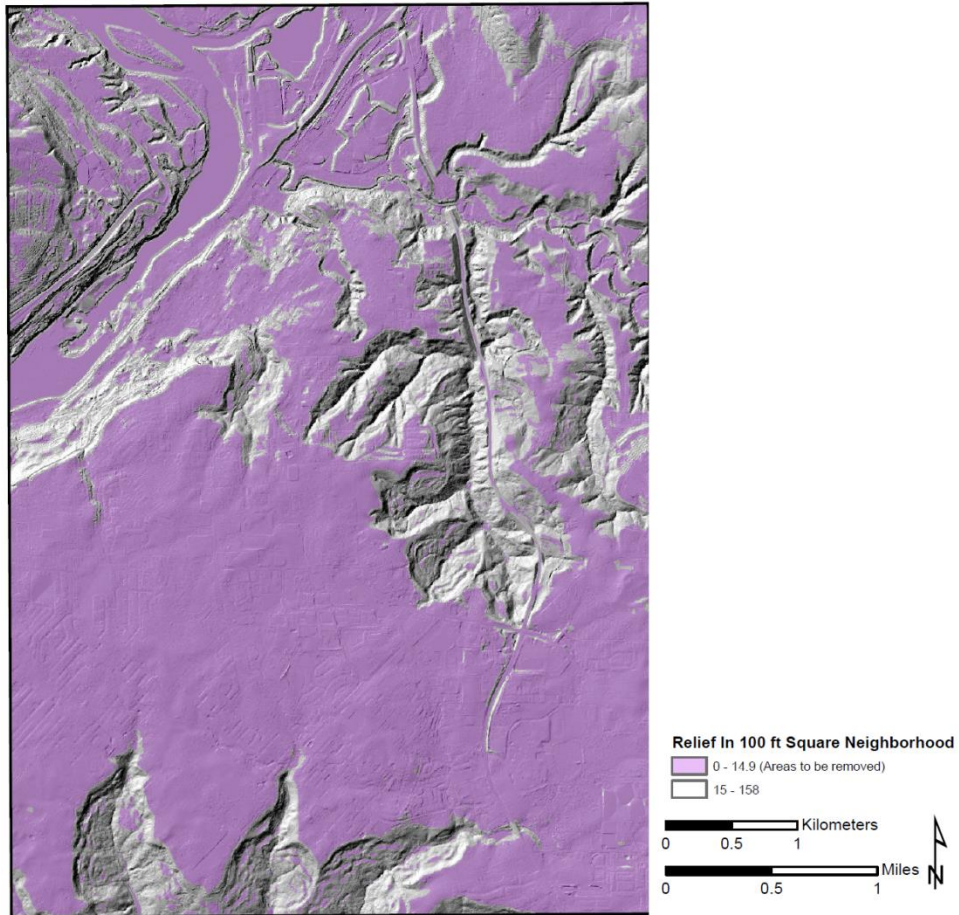
In the remaining areas, we assume that the pre-failure slope angles reflect the characteristic values at which the material in each engineering geologic unit fails, so we can use statistics on the pre-failure slopes to determine the critical slope value for each unit. We start by joining the landslide inventory attributes to the engineering geology polygons. Next, we calculate the mean and standard deviation (STD) of the slope angle for each engineering geology polygon. We will use the mean and two sets of standard deviation values (both −1 STD and −2 STD), as they are standard statistical divisions and they divide the dataset into three groups, which we can use to represent our three categories (low, moderate, high) (**Figure 3.18**):
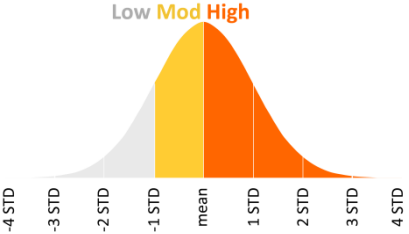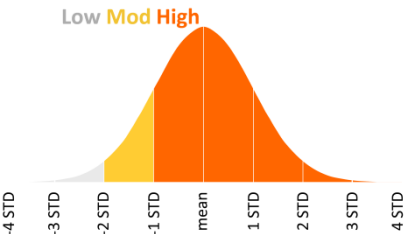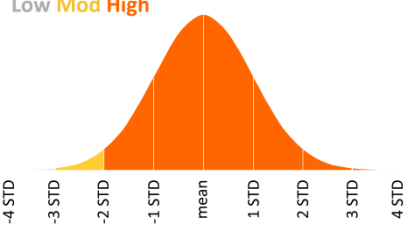
- Mean: the average value. In a standard normal distribution dataset, greater than or equal to the mean is slightly more than 50% of the data.
- −1 STD: 34.1% less than the mean. In a standard normal distribution dataset, greater than −1 STD is 84.1% of the data or the majority of the data.
- −2 STD: 47.7% less than the mean. In a standard normal distribution dataset, greater than −2 STD is 97.7% of the data or almost all of the data.

Figure 3.18. Graphical representation of the statistical divisions in a normal distribution.
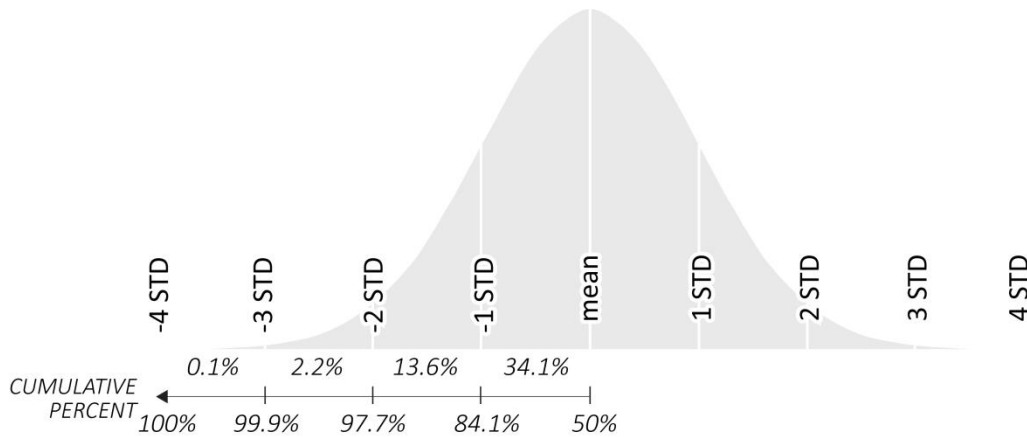
To determine which divisions (i.e., the mean, and one or two standard deviations) were most suitable for the thresholds between the low, moderate, and high susceptible slope classes, we tested three scenarios of the percent of pre-failure slope values captured by the final deep landslide susceptibility zones versus the percent of the landscape covered by the classes (**Table 3-3**). The goal was to maximize the percent of pre-failure slope angles captured and at the same time not dramatically increase the percent of study extent covered by the modeled high susceptible slope class.

Table 3-3.   Results of scenario testing of the percentage of pre-failure slope values captured in the susceptible slope classes versus the percentage of the study area covered by the susceptible slope classes for all geologic engineering units in the Oregon City quarter quadrangle shown in Figure 3.9.

	Susceptible Slope Class	Statistical Division	Percentage of Pre-Failure Slope Values Captured	Percentage of Study Area Covered
Scenario 1				
	2 (High)	greater than or equal to the mean	50.0%	11.1%
	1 (Moderate)	greater than or equal to −1 STD and less than the mean	34.1%	6.9%
	0 (Low)	less than −1 STD	15.9%	82.0%
Scenario 2				
	2 (High)	greater than or equal to −1 STD	84.1%	18.0%
	1 (Moderate)	greater than or equal to −2 STD and less than −1 STD	13.6%	11.8%
	0 (Low)	less than −2 STD	2.3%	70.2%
Scenario 3				
	2 (High)	greater than or equal to −2 STD	97.7%	29.8%
	1 (Moderate)	greater than or equal to −3 STD and less than −2 STD	2.1%	35.9%
	0 (Low)	less than −3 STD	0.2%	34.2%

Mean = 19.07, STD = standard deviation = 5.58.

Scenario 2 (**Table 3-3**) appears be best for capturing the largest percentage of pre-failure slope angles (84%), while maintaining a relatively low percentage of coverage by the high susceptible slope class (18%) and a relatively large percentage of coverage by the low susceptible slope class (70%). Therefore, we selected the statistical division values in scenario 2 as the threshold to separate the low, moderate, and high susceptible slope classes. In the geodatabase, slopes greater than or equal to −1 STD get a slope class score of 2 (high), slopes greater than or equal to −2 STD and less than −1 STD get a score of 1 (moderate), and remaining values (less than −2 STD) get a score of 0 (low). **Figure 3.19** (left) shows how these divisions look on a map, while **Figure 3.19** (right) shows the same map after removal of the low relief area from the susceptible slope score map (purple area in **Figure 3.17**).

Figure 3.19. Map of susceptible slope scores: 0 (no color, gray), 1 (orange), and 2 (red). Landslides are outlined in black; (left) raw output, (right) areas of very low relief removed. The areas shown correspond to the Oregon City quarter quadrangle shown in Figure 3.2.

Methodology progress bar:	High Susceptibility	⟹	Moderate Susceptibility ▼	⟹	Low Susceptibility
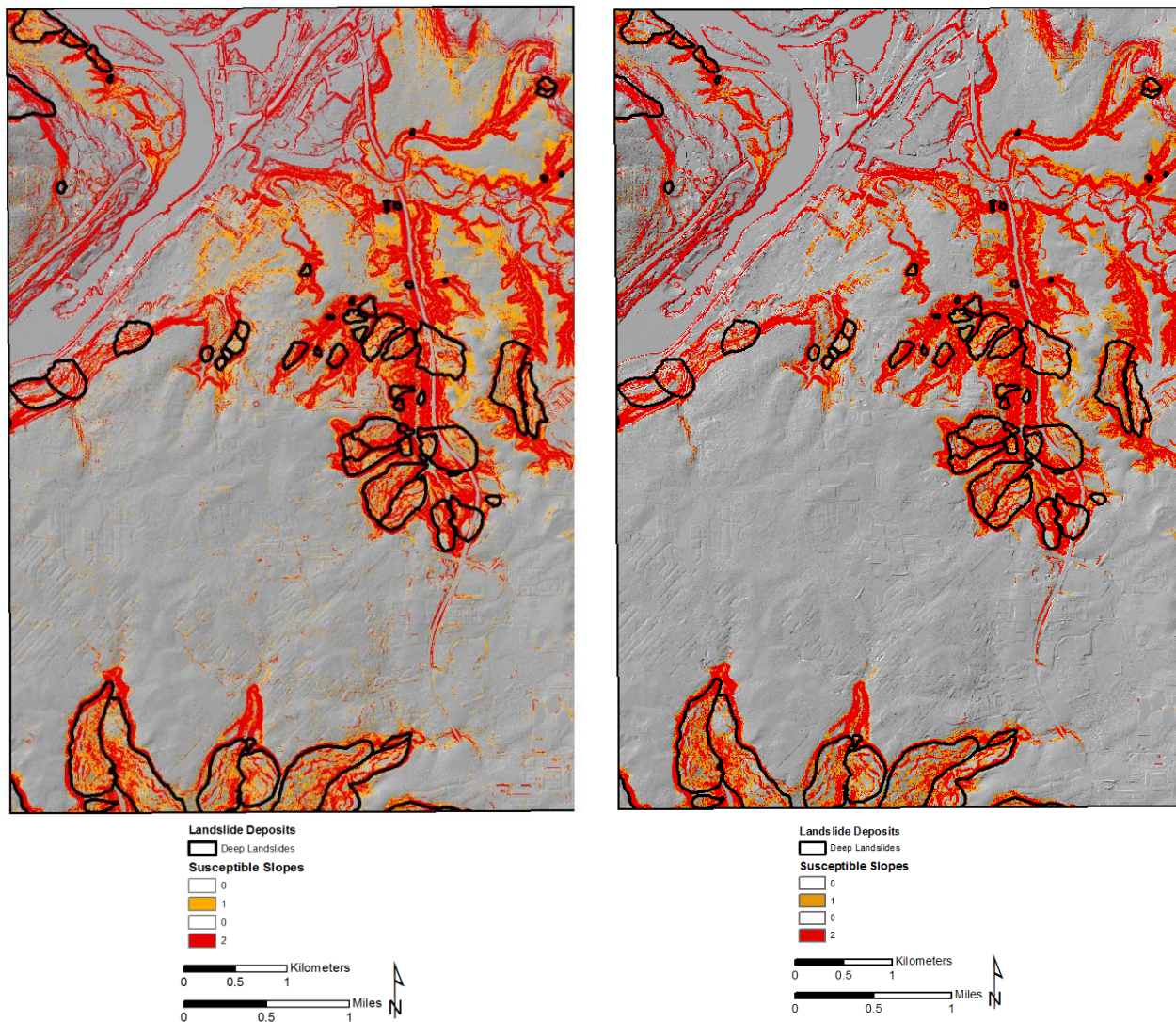
Preferred Direction of Movement

The forth factor influencing the moderate susceptibility zone buffer is preferred, or susceptible, direction of movement of landslides. Deep landslides tend to slide along bedding planes in the direction of the dip, so a standard factor to examine in site-specific landslide evaluations is geologic structure, including bedding dip and dip direction (Lane, 1987; Roering and others, 2005). Subsurface geologic structure can be difficult to assess. Readily available digital information about geologic structure is commonly incomplete; for example, there is no strike and dip information in the statewide geologic data compilation for Oregon (OGDC-5; Ma and others, 2009).

However, landslide inventories completed by following DOGAMI SP-42 include direction of movement at every landslide. Because we do not have a spatially dense collection of digital strike and dip measurements throughout Oregon, we use the recorded direction of movement from the landslide inventory database along with any readily available strike and dip locations to evaluate preferred direction of movement. We compare the aspects of local slopes to the preferred direction of movement. We give scores of 0, 1, or 2 to the result, depending on how well the orientations of the aspects and preferred directions match at any particular location.

To accomplish this, we first convert landslide polygons to points attributed with the landslide direction of movement. We use the vertices of the landslide deposit polygon as the locations for the points. These points are similar to locations of strike and dip. Then we add structural points (such as strike and dip) to this point dataset (**Figure 3.20**). We attribute each point (landslide or structure) with an azimuth direction rounded to the nearest 22.5 degrees (see Burns and Madin, 2009a).

Figure 3.20. Map of landslide direction points and structure points. The area shown corresponds to the Oregon City quarter quadrangle shown in Figure 3.2.
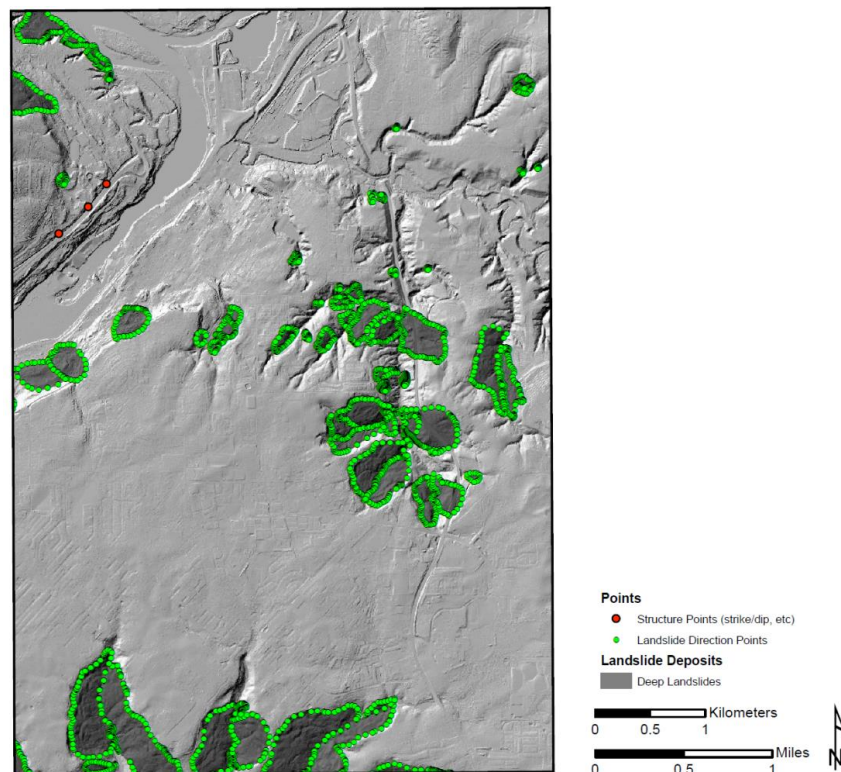
We then convert these points to raster with 3 ft^2 (~1 m^2) cells (**Figure 3.21)** by using inverse distance weighting (IDW) with a maximum distance of 1,000 ft (305 m). We chose this value by examining the data in SLIDO 4.0 (Burns, in press). There are 9,126 deep landslides in the SLIDO 4.0 database (Burns, in press). The *mean* area of these deep landslides is 895,259 ft^2 (83,172 m^2). If we assume most of the landslides have relatively similar lengths and widths, we obtain a square of approximately 1,000 ft^2 (305 m^2).

Figure 3.21. Preferred direction map of the triangulated irregular network (TIN) created from direction points (small red and green dots) with inverse distance weighting (IDW) set to 1,000-ft^2. The area shown corresponds to the Oregon City quarter quadrangle shown in Figure 3.2.
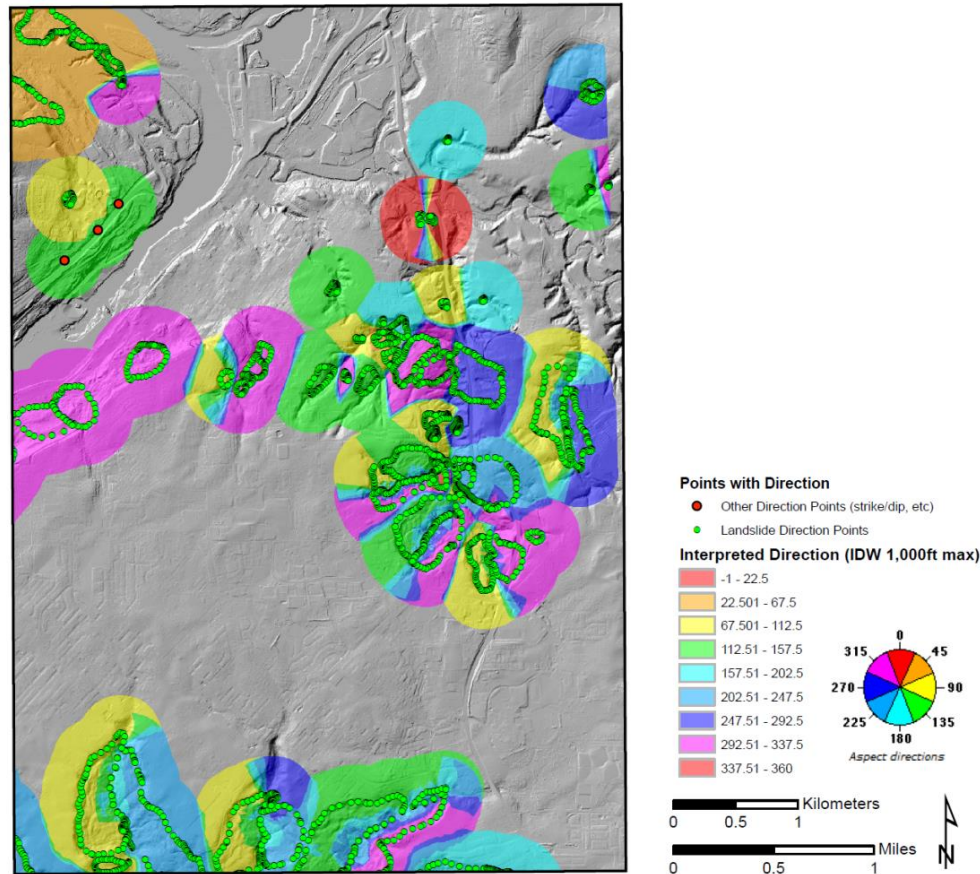
Next, we convert the lidar DEM (3 ft^2 resolution) to an aspect map (**Figure 3.22**). When the DEMs are converted to an aspect map with such high resolution, fine-scale topographic features can result in aspects divergent from and even 180 degrees from the overall generalized slope aspect (**Figure 3.22**). We tested smoothing the DEM from 3 ft^2 grids to 15 ft^2 grids to see if the overall slope aspect was improved, as it was for susceptible slopes (see section **3.3.2.2.3**). In our test area, the mean slope aspect changed from 261 degrees with a standard deviation of 67 to a mean slope aspect of 270 degrees with a standard deviation of 55. We deemed this not enough of an improvement to warrant the change in cell size, especially given that the slope aspect is generalized into 45-degree wedges (see legend in **Figure 3.22**). While changing the cell size make no improvement, we must reclassify the ten Esri default aspect classes in the aspect maps (the preferred direction map and slope aspect map), to eight generalized classes by removing the Flat class and combining the North classes (**Figure 3.23**).

Figure 3.22. Map of the aspect from the lidar DEM (3 ft^2 resolution) produced by the 10 Esri default aspect classes. Landslides are outlined in black. The area shown corresponds to the Oregon City quarter quadrangle shown in Figure 3.2.
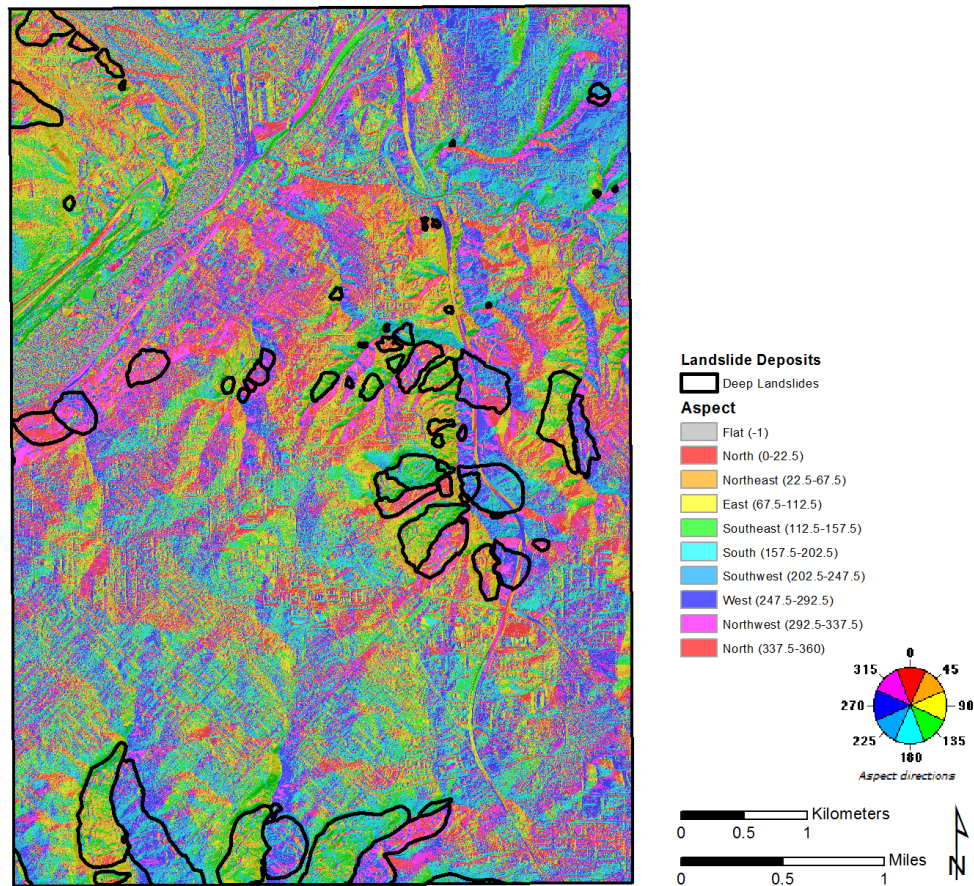
Figure 3.23. Eight generalized aspect classes for preferred direction of movement after converting from the default Esri result.
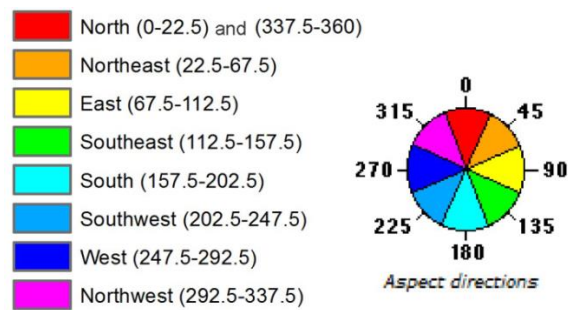
Finally, we use the raster calculator to evaluate where the following situations occur and assign scores:

- If the aspect map is equal to the preferred direction map class (for example, preferred direction = 90 and the aspect map = 90), set the score = 2.
- If the aspect map is one class less than or one class larger than the preferred direction map (for example, preferred direction = 90 and the aspect map = 45 or 135), set the score = 1.
- For all other areas, set the score = 0.

We then combine the three score maps to create the final preferred direction of movement score map (**Figure 3.24**).

Figure 3.24. Map of the preferred direction of movement factor with scores of 0 (no color, gray), 1 (yellow), and 2 (orange). Landslides are shown in black. The area shown corresponds to the Oregon City quarter quadrangle shown in Figure 3.2.
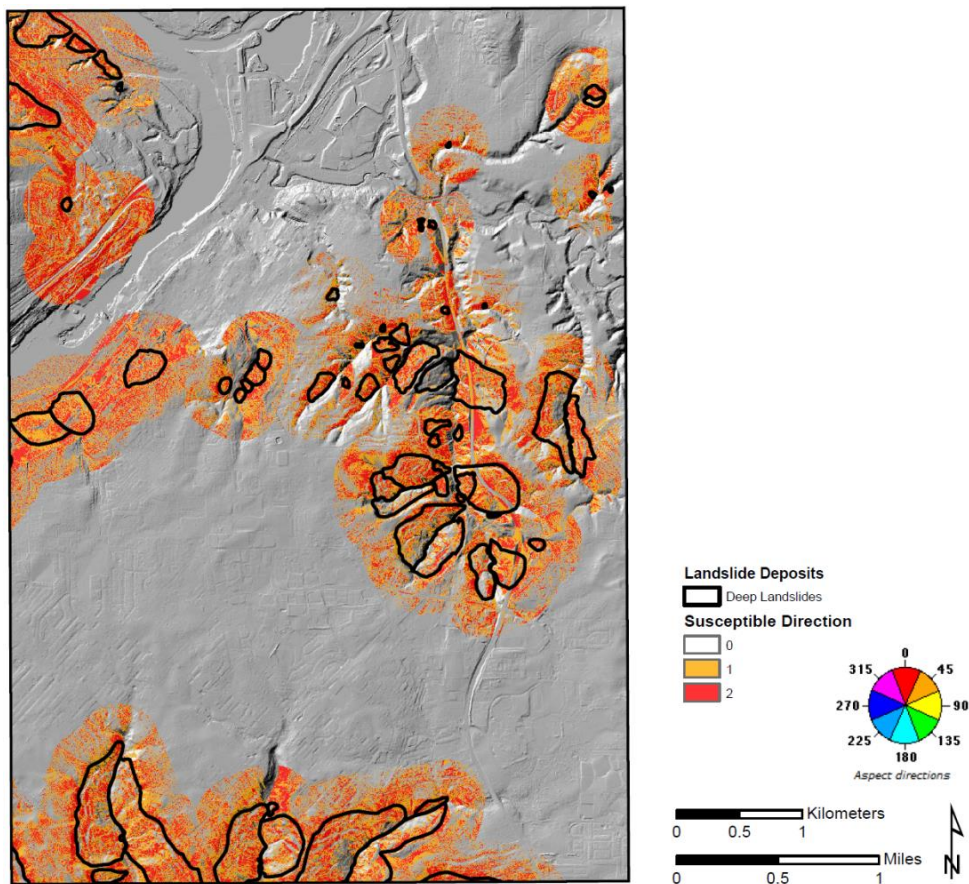
3.3.2.2.4   Combined Moderate Factors Score

We now have four raster maps, one for each of the four factors: susceptible geologic units, susceptible geologic contacts, susceptible slope angles, and preferred direction of movement. We develop the combined moderate factors score layer by adding together the scores for each of the factors. Each individual factor raster has scores of 0, 1, or 2, so the final combined map will have a range of values from 0 to 8. Zero means none of the factors were present at a particular site, while 8 means the "high" value for each of the four factors was present at a particular site (Figure 3.25). We give each factor the same weight because we do not have any data to assess the influence of each factor. Collecting and incorporating such data would improve the protocol.

Figure 3.25. Final combined moderate factors score map. The area shown corresponds to the Oregon City quarter quadrangle shown in Figure 3.2.
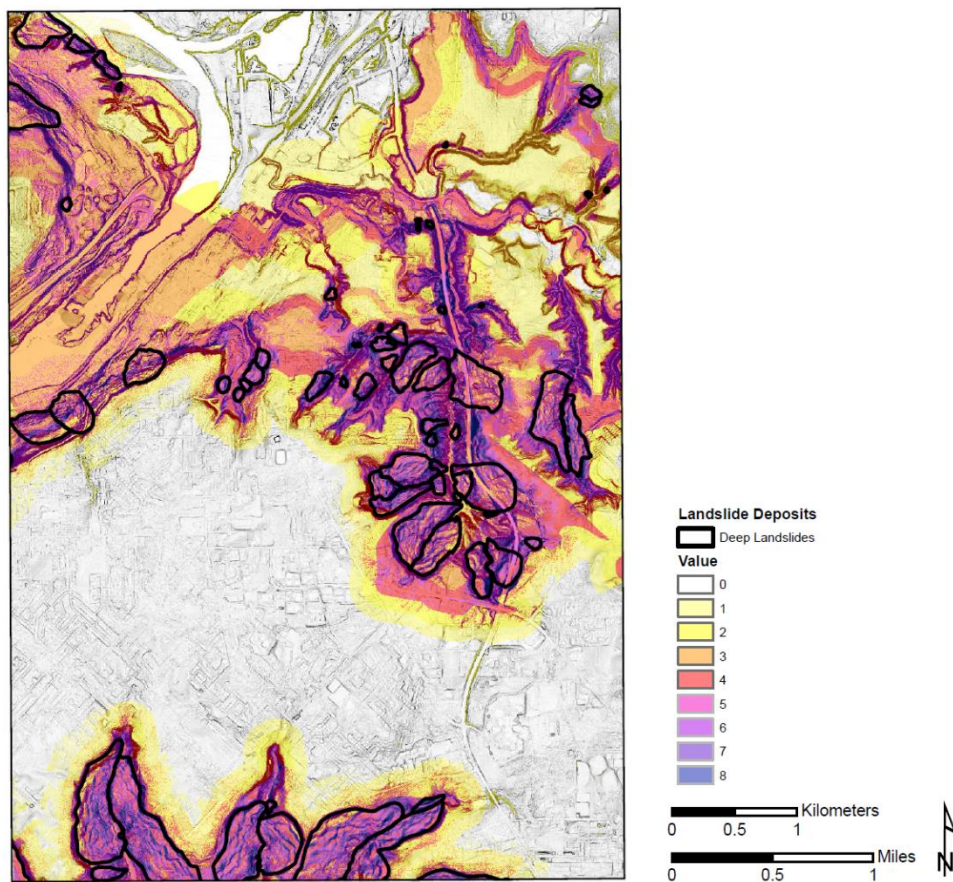
3.3.3 Delineating the Moderate Susceptibility Zone

We delineate the final moderate susceptibility zone by expanding the minimal moderate susceptibility zone (sections **3.3.1** and **Figure 3.7**). To expand the zone, we apply a number of subjective factors to the combined moderate factors score map in order to draw "by hand" the final line between the moderate susceptibility zone and the low susceptibility zone. These subjective factors are discussed below.

After a number of tests (see section **4.0** for a discussion of the methods and results of the testing) we concluded that as a general rule the best value for the boundary between the moderate and low susceptibility zones is ≥ 4. However, we recommend that an experienced geologist draw the boundary line (**Figure 3.26**) using values between 3 and 5 as a guide while considering the following subjective factors:

- Include small areas (mostly islands) of low combined moderate factors scores (3 or less) surrounded by consistently higher (5+) scores. An example can be seen in the northeast part of **Figure 3.26** where a small island of score 0 is surrounded by higher scores and was included in the final moderate susceptibility zone.
- Exclude relatively flat areas with consistent scores of at least 3 but that have few or no scores greater than 4. An example can be seen in the northwest part of **Figure 3.26** where there are extensive areas of scores 3 and 4.
- Exclude very small isolated or peninsula areas with moderate to high combined moderate factors scores (4+).

The main reason for drawing the final line by hand is to eliminate isolated cells or small groups of cells ("islands") with low scores that are surrounded by moderate or high susceptibility. This is more important with deep landslides than with shallow landslides, because deep slides tend to be much larger and commonly contain areas of very low slope.

Figure 3.26. Map showing the hand-drawn line (black) between the moderate and low susceptibility zones. Also shown are the high susceptibility zone (red), the combined moderate factors score (yellow to blue areas), and the minimal moderate zone (solid orange). The area shown corresponds to the Oregon City quarter quadrangle shown in Figure 3.2.
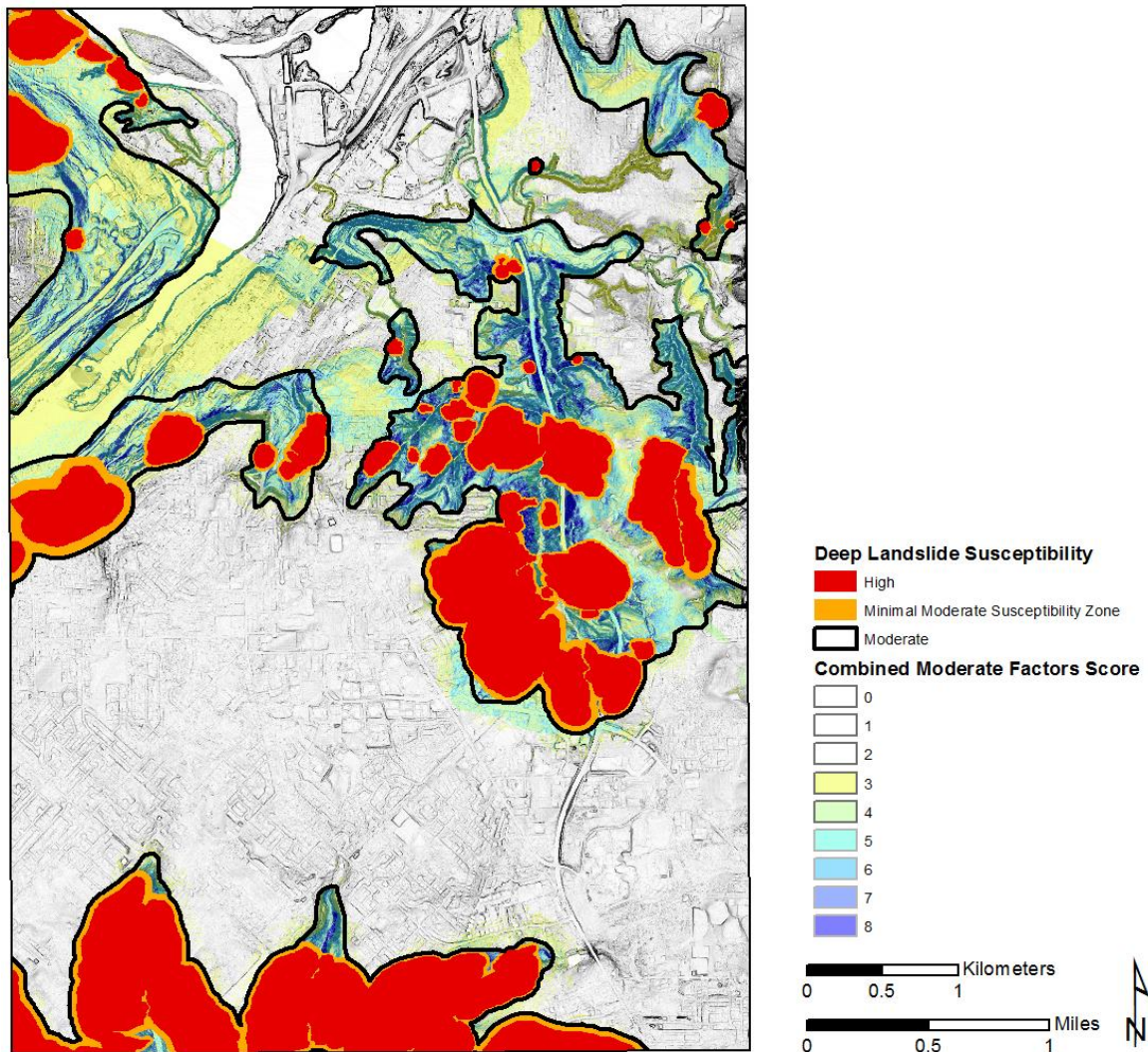
To summarize, the minimal moderate susceptibility zone layer plus the combined moderate factors score map layer with its hand delineated lower boundary make up the final deep landslide moderate susceptibility zone layer.

Methodology progress bar: | High Susceptibility ⇒ Moderate Susceptibility ⇒ Low Susceptibility ▼

3.4 Low Susceptibility Zone

The low zone simply consists of areas not identified as high or moderate zones.

3.5 Final Deep Landslide Susceptibility Map

The final deep landslide susceptibility map shows high, moderate, and low zones (**Figure 3.27**). The high susceptibility zone consists of landslide deposit polygons and head scarp-flank polygons with her head scarp-flank polygon buffers (section **3.2**). The moderate susceptibility zone consists of a minimal moderate zone polygon and a layer created by combining four geologic factor rasters to expand the minimal moderate zone (section **3.3**). The low zone consists of areas not identified as high or moderate zones.

Figure 3.27. Map of high (red), moderate (orange), and low (gray) deep landslide susceptibility zones. The area shown corresponds to the Oregon City quarter quadrangle shown in Figure 3.2.
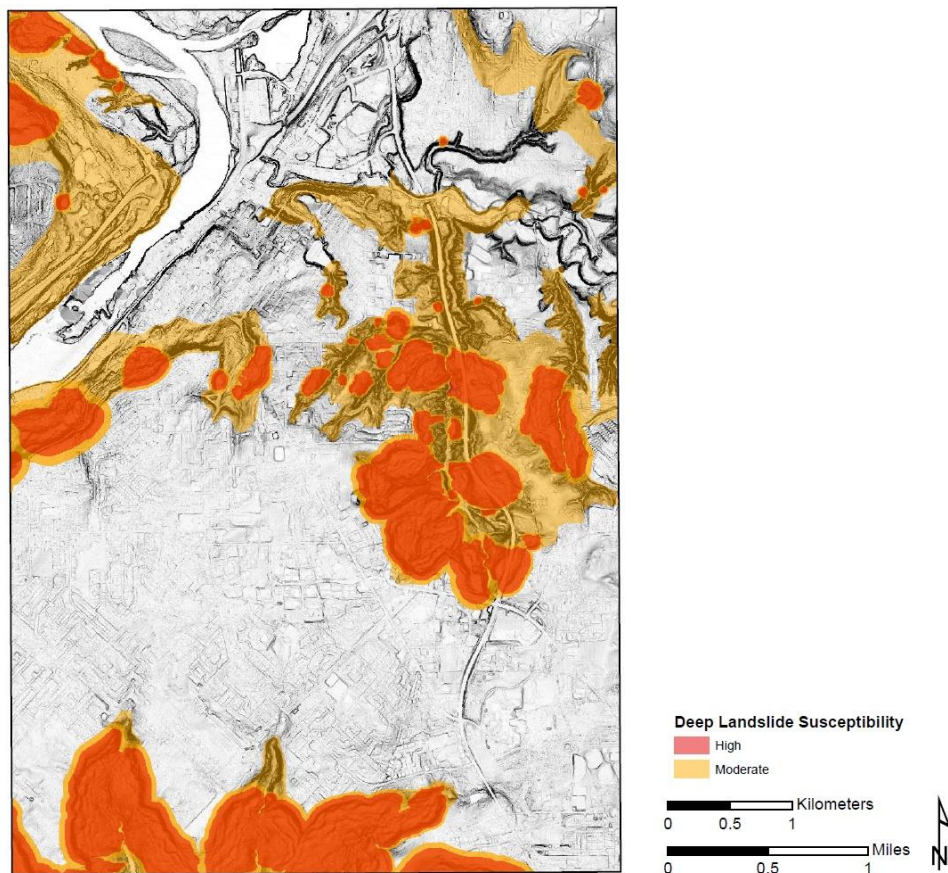
4.0 DEEP LANDSLIDE SUSCEPTIBILITY HAZARD MAP EFFECTIVENESS

The objective of a deep landslide susceptibility map is to create an area that minimizes moderate and high susceptibility hazard zones but that at the same time encompasses all future deep landslides (Godt and others, 2008). For example, a susceptibility map that captures 100% of the deep landslides in a particular area but also maps the entire area as high hazard zone is overly conservative. While this conservative approach accomplishes one hazard mapping goal—predicting areas of future landslide occurrence—the approach almost completely fails at a second goal—predicting which areas are not expected to have future landslides. Our objective was to maximize both of these goals.

The best way to test our method would be new deep landsliding events in an area we had already mapped with this protocol. However, deep landslides are not common in the short term (e.g., annually) in Oregon. The chance of a deep landslide occurring during the development of this protocol and in the few areas of the state we have mapped using this protocol is extremely low.

The other difficult part of testing this method is that all known deep landslides are already being used as part of our protocol input data to predict susceptibility and should not be used to test the method results. Therefore, we need to construct an artificial data set for testing. Landslide inventories that classify landslides as either prehistoric or historic provide a natural separation into two subsets of data. The question is, can one of these subsets be used to test the effectiveness of the protocol?

Many active (historic) deep landslides in the Pacific Northwest are reactivations of all or parts of existing prehistoric landslides (Giraud and Shaw, 2007). Recall from section 2.2 that approximately 25% of historic landslides in SLIDO 3.2 intersect with prehistoric landslides and approximately 70% of prehistoric landslides intersect with other existing landslides (Burns, 2014). Therefore, our approach was to extract all historic landslides from the original dataset, leaving the prehistoric landslide set as a "full" data set, and use the historic set as the "test" set. We then re-modeled deep landslide susceptibility using only the prehistoric landslide data. Using the separate historic "test" set as "future" landslides, we could inspect the hazard maps to see how well they captured the "future" landslides. This approach, while not independent, allowed us to test the method. The area we chose to test the protocol's effectiveness was the Bull Run Watershed, where we had already used this protocol to map deep landslide susceptibility (Burns and others, 2015).

4.1 Bull Run Watershed Map Test

4.1.1 Study Area and Previous Work

The Bull Run watershed is the primary drinking water supply for the City of Portland, Oregon; hundreds of thousands of people rely on the water supply. The watershed is managed by the Portland Water Bureau. The watershed area is approximately 140 mi^2 (363 km^2) and is located 25 mi (40 km) east of downtown Portland.

We chose Bull Run Watershed for our test area because several historic deep landslides have been mapped there and because we had recently completed a project with the City of Portland Water Bureau (PWB) to examine the landslide hazard in the watershed (Burns and others, 2015). For that project we created a landslide inventory as well as shallow and deep landslide susceptibility maps. We used the deep landslide susceptibility protocol presented in this paper to create the deep landslide susceptibility map.

During the Bull Run Watershed mapping project, Burns and others (2015) located 80 historic deep landslides and 380 prehistoric deep landslides (**Figure 4.1**) to create a landslide inventory. The total area of prehistoric landslides, excluding overlap, covered approximately 11% of the watershed, while the total area of historic landslides covered approximately 0.5%. They also mapped 11 bedrock engineering geologic map units.

Figure 4.1. Map of the Bull Run Watershed extent showing 80 historic and 380 pre-historic deep landslides.
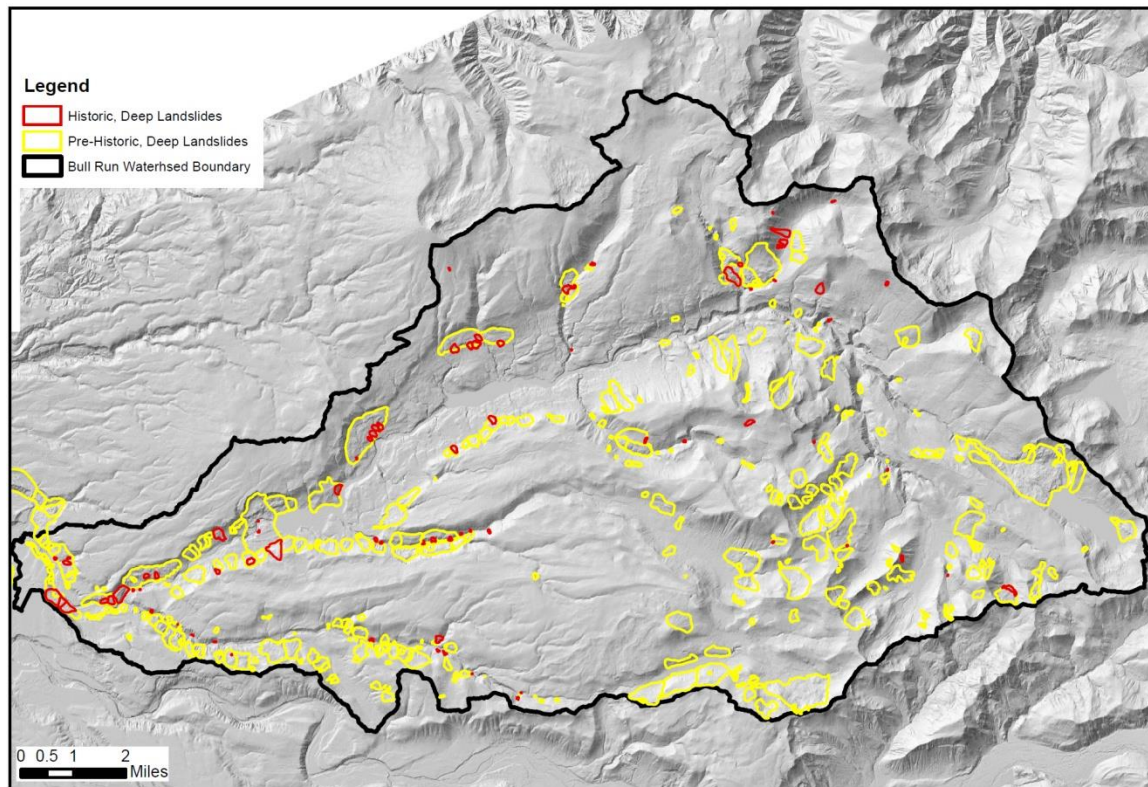
4.1.2 Deep landslide Susceptibility Test and Results

With the Bull Run data, we were ready to test the goals of the protocol—predicting future landslide occurrence and predicting which areas are not expected to have landslides. First, we extracted the *historic* landslide subset from the Bull Run Watershed landslide inventory (Burns and others, 2015), leaving the *prehistoric* landslide subset for our test. Then we remodeled the area using just the prehistoric landslide subset to create new landslide susceptibility zones.

We explored the effectiveness of the new zones through two scenarios. In the first scenario, to test for goal 1, we examined how well the high zone and the minimal moderate zone buffer (a portion of the moderate zone) captured the omitted historic landslides. We did this by overlaying the historic landslide inventory on the susceptibility zones made only from prehistoric landslide data (**Figure 4.2**).

Figure 4.2. Goal 1, test scenario 1: Map of prehistoric landslides, high landslide susceptibility zone, and the minimal moderate buffer zone portion of the moderate susceptibility zone made from only the prehistoric landslide data, with an overlay of the omitted historic landslide extents. Larger scale map (bottom) is detail of central western portion of the small-scale map (top).
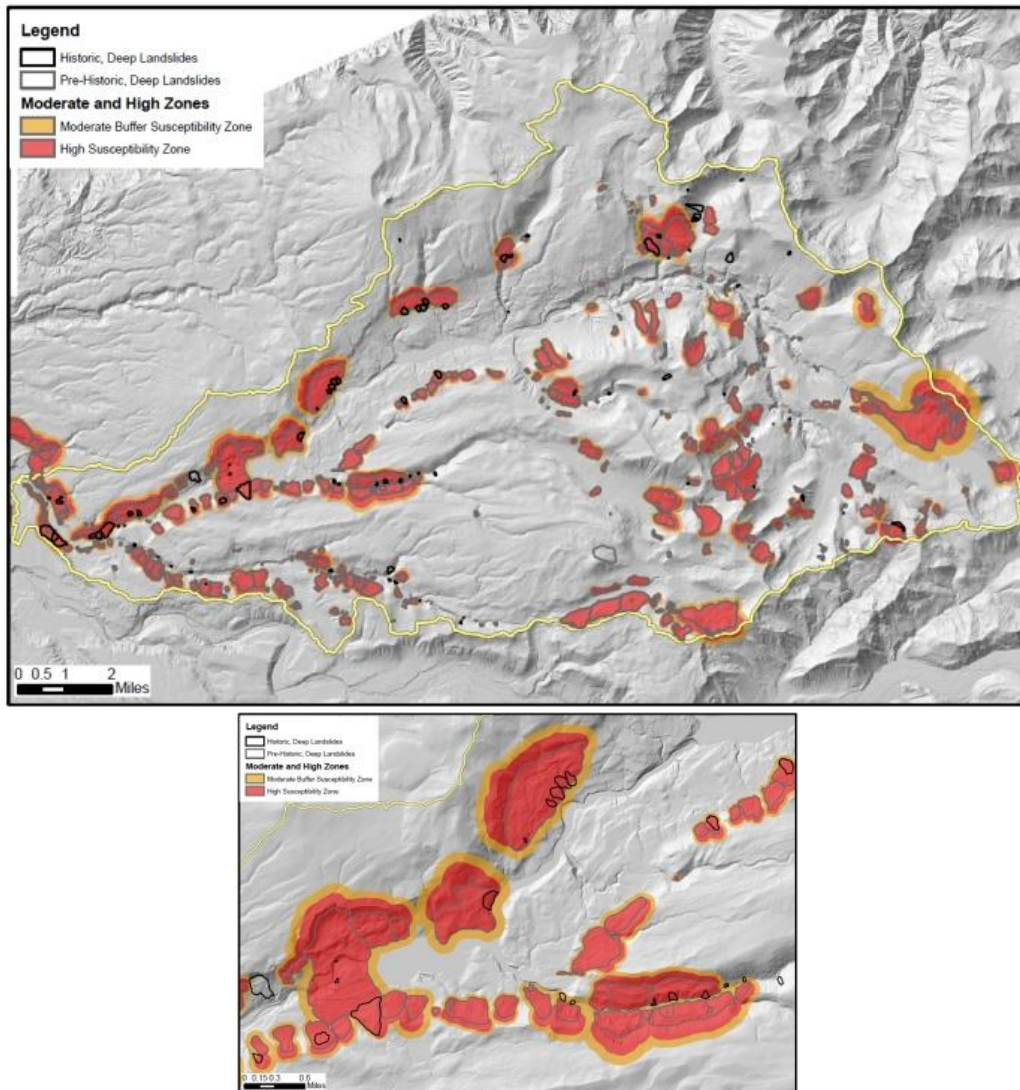
In the second scenario, again to test for goal 1, we overlaid the historic landslide inventory on the new combined moderate factors zone to examine how well each of the classes (0 to 8) in the combined moderate factors score captured deep landslides (**Figure 4.3**).

Figure 4.3. **Goal 1, test scenario 2: Map of prehistoric landslides and the combined moderate factor scores made from only the prehistoric landslide data, with an overlay of the omitted historic landslide extents.**
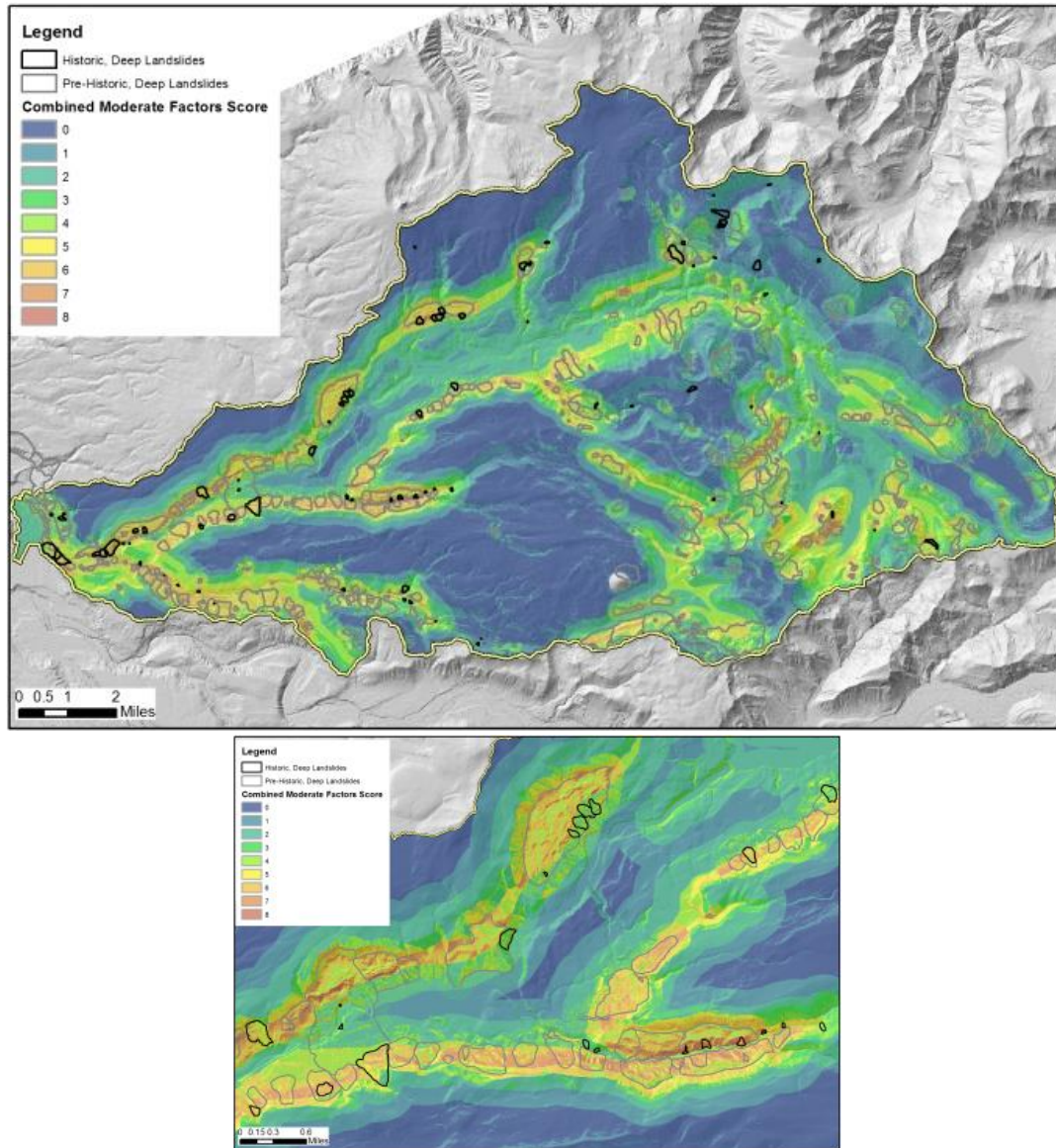
To predict locations that should *not* have future landslides (goal 2), we examined the same overlays created for goal 1, then calculated the percentage of the entire watershed covered by the datasets. The results of this examination are summarized in **Table 4-1** and are displayed in **Figure 4.4**.

Table 4-1. Summary showing deep landslide susceptibility protocol results using only prehistoric landslide data as input.

		Goal 1				Goal 2
		Historic Landslide Coverage (sq ft)	Historic Landslide Coverage (%)	Historic Landslides Touched (Count)	Historic Landslides Touched (%)	Entire Watershed Coverage (%)
	High susceptibility zone	14,672,097	71%	40	50%	14
Scenario 1	High susceptibility zone and combined minimal moderate buffer zone	15,876,225	77%	57	71%	21%
Scenario 2	Combined moderate factors score					
	0–8	20,129,688	98%	80	100%	100%
	1–8	19,373,562	94%	80	100%	82%
	2–8	17,974,746	87%	80	100%	76%
	3–8	16,817,022	82%	68	85%	51%
	4–8	15,195,582	74%	68	85%	35%
	5–8	10,922,598	53%	60	75%	19%
	6–8	7,225,479	35%	56	70%	10%
	7–8	3,384,810	16%	39	49%	4%
	8–8	913,905	4%	35	44%	1%

Figure 4.4. Plot of percent of watershed coverage versus historic landslide coverage.
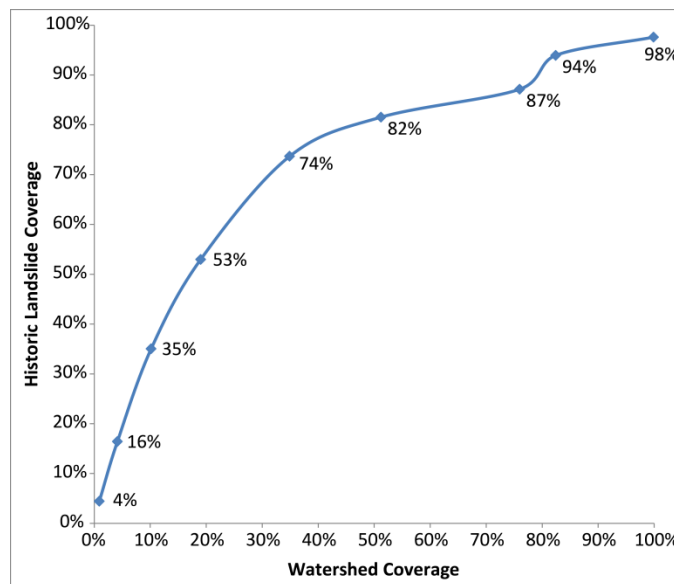
As displayed in **Figure 4.2** and **Figure 4.3** and summarized in **Figure 4.4** and **Table 4-1**, together the high zone and the minimal moderate buffer zone (scenario 1) capture 77% of the total area of historic landslides but cover only 21% of the total watershed. This indicates a high level of effectiveness for goal 1.

However, because goal 1 is to capture the maximum area of historic landslides in both the high zone and in the entire moderate zone, the high and minimal moderate buffer zones (scenario 1) cannot be used alone: only 40% of the historic landslides are touched by the hazard zone, excluding 60% of historic landslides. Therefore, we must use the combined moderate factors score to assist in capture. The combined moderate factors score dataset (scenario 2) increases coverage of historic landslides steadily up to a score of ≥4 (~74%) (**Figure 4.4**). Above 74%, however, a minor increase in landslide coverage corresponds with significant increase in watershed coverage. Furthermore, at ~74% landslide coverage, watershed coverage is 35%, far more than the 11% area covered by pre-historic deep landslides in the landslide inventory. Accordingly, a score of ≥4 (i.e., 74% landslide coverage and 35% watershed coverage) seems like the best value both to capture landslides and to reduce overestimation. However, recall that expert judgment is required to map the line between the moderate and low susceptibility zones and could result in the moderate zone line drawn at a score of 5 or a score of 3 in some locations (see **Figure 3.26**).

## 4.2 Comparison of Protocol Results to Other Landslide Susceptibility Maps

The effectiveness of the map made using the protocol defined in this paper may be visually compared to results from other deep landslide susceptibility mapping projects in the same area. One project that generated deep landslide susceptibility maps following the general deep landslide susceptibility protocol described in this paper was in Clackamas County (Burns and others, 2013). The Clackamas County project area spatially overlaps three other recent landslide susceptibility mapping efforts that followed different methods:

- Landslide susceptibility analysis of lifeline routes in the Oregon Coast Range (Santha-Mahlingham and others, 2015)
- Ground motion, ground deformation, tsunami inundation, coseismic subsidence, and damage potential maps for the 2012 Oregon Resilience Plan for Cascadia Subduction Zone Earthquakes (Madin and Burns, 2013)
- Statewide landslide susceptibility overview map of Oregon (Burns and Mickelson, 2016)

Because of this overlap we can visually compare results of these maps. We were not able to perform quantitative analysis, because the methods used to create the four maps differed. To visually compare the maps, we converted the susceptibility zones shown in these maps to the zones for our deep landslide susceptibility map as follows. The Santha-Mahlingham and others (2015) map originally defined very low, low, moderate, high, and very high zones. To compare that map with our map, we combined the very low and low zones into the low zone, and we combined the high and very high zones into the high zone. The Madin and Burns (2013) map was originally classified with the 0 to 10 Hazus classification scheme (FEMA, 2011); we used the conversion outlined by Burns and others (2008) to reclassify the Hazus zones to high, moderate, and low. The Burns and Mickelson (2016) map was originally classified with low, moderate, high, and very high; we combined high and very high into high. **Figure 4.5** shows representative areas from the reclassified maps in an area where these three maps overlap the Burns and others (2013) study that followed the present protocol.

Several notable differences can be seen in **Figure 4.5**. The Madin and Burns (2013) map (**Figure 4.5D**) seems to significantly overestimate the spatial extent of the hazard given the mapped landslide inventory. The Santha-Mahlingham and others (2015) map (**Figure 4.5E**) appears to not overestimate the spatial extent of the hazard but does not capture all mapped landslides. Again, because the methods used to create the susceptibility maps differed from the present method, we did not do any quantitative analysis. However, of these four maps, the protocol described in this paper appears to both maximize landslide capture and minimize the area of susceptibility.

Figure 4.5.   Comparison of deep landslide susceptibility mapping in an area of Clackamas County, Oregon. Panels A-E show landslide polygons as black outlines. (B) Map shows deep landslide susceptibility protocol zones created following the protocol in this paper. The three other maps (C-E) show existing deep landslide susceptibility zones from (C) Burns and Mickelson (2016), (D) Madin and Burns (2013), and (E) Santha-Mahlingham and others (2015) reclassified using the classification scheme of this protocol. See the text for the reclassification procedure.
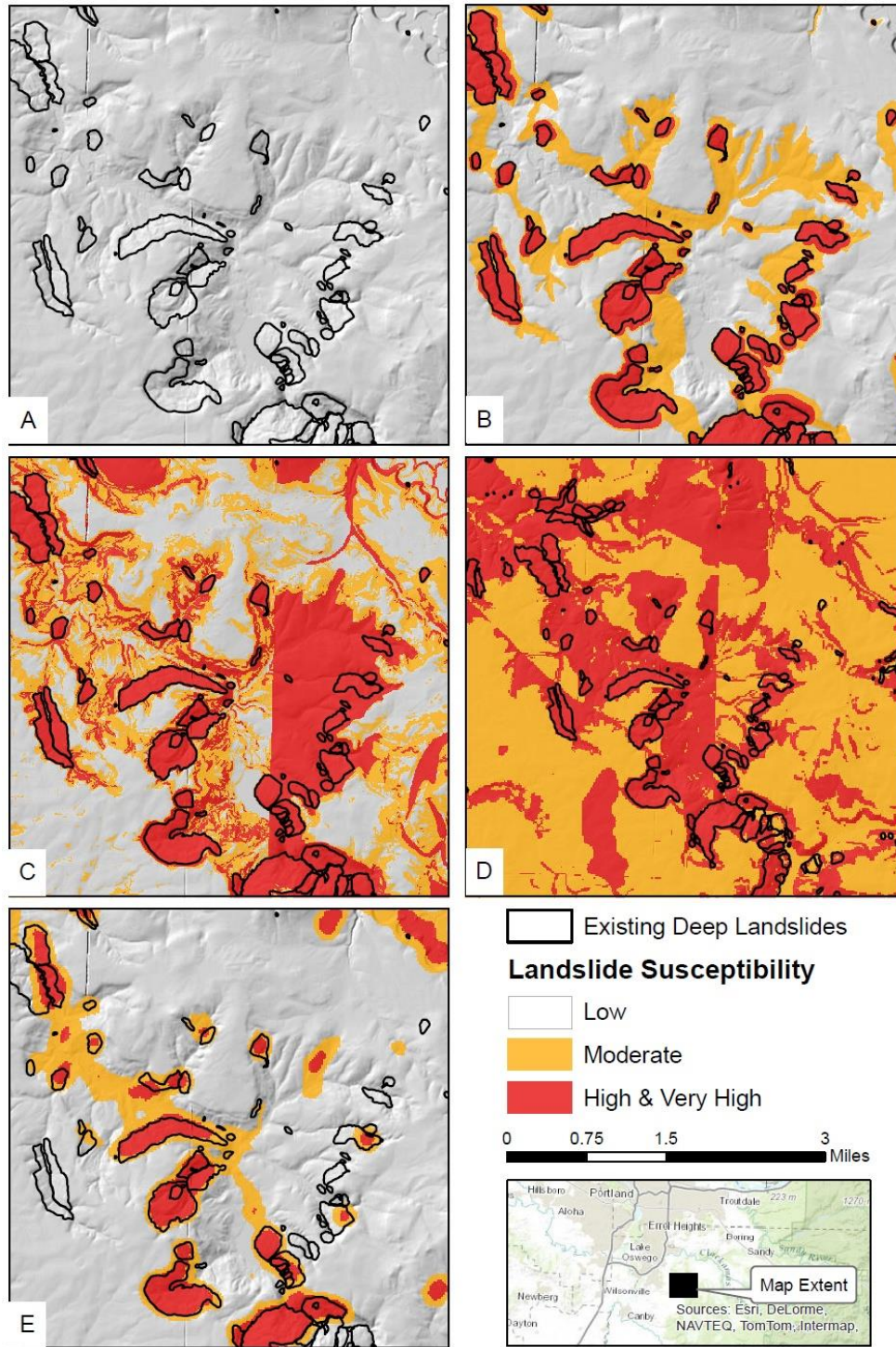
5.0   DEEP LANDSLIDE SUSCEPTIBILITY MAP TEMPLATE

We developed a 1:8,000 scale map template to display deep landslide susceptibility zones. **Figure 5.1** shows the template applied to the example Oregon City data used in this paper. The map template provides a means to display data in a consistent manner for any area in Oregon.

Figure 5.1.   Example deep landslide susceptibility map: northwest quarter of the 7.5 minute USGS Oregon City quadrangle (Burns and others, 2013).
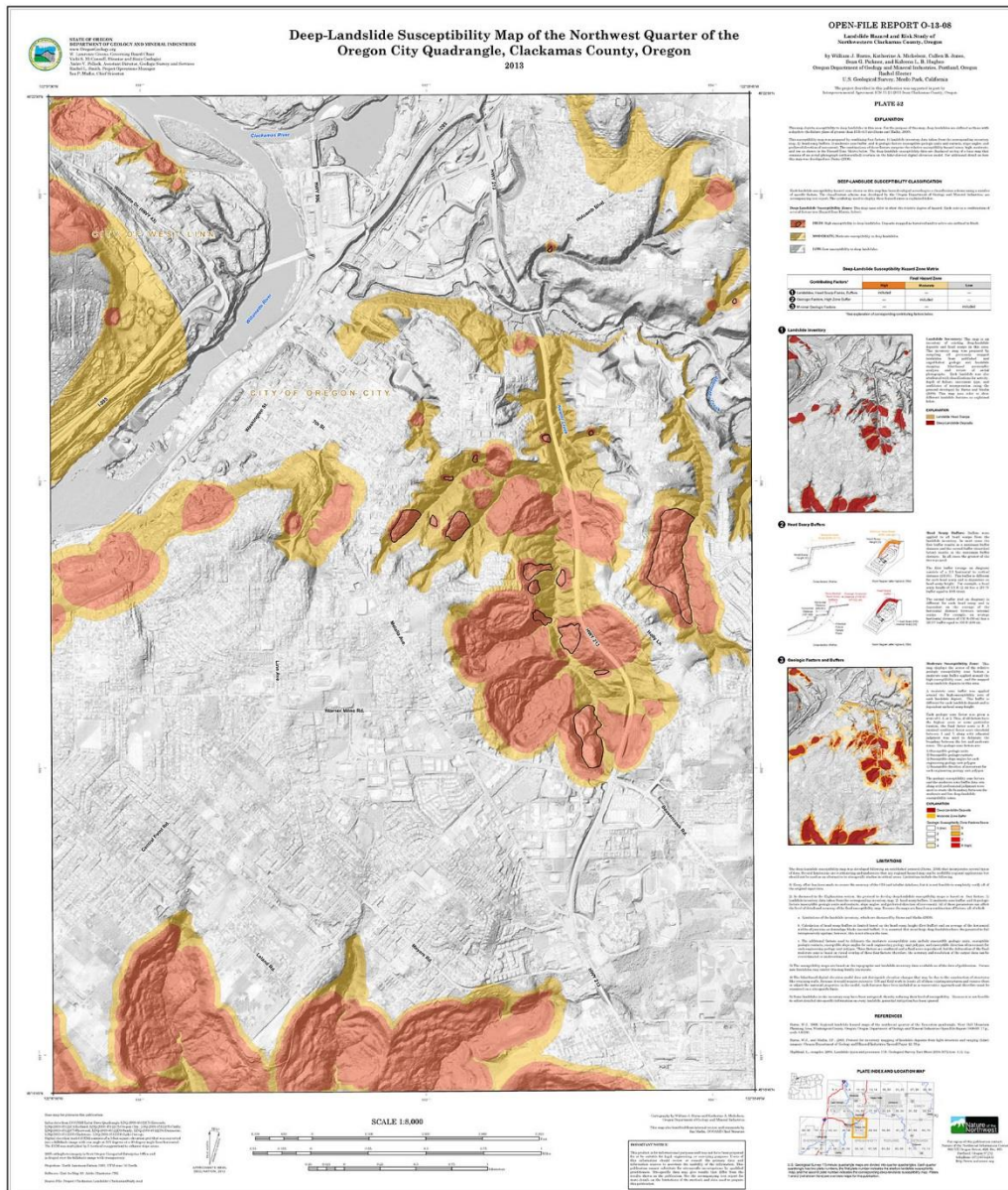
6.0   LIMITATIONS OF THE PROTOCOL

The limitations of the deep landslide susceptibility mapping protocol are listed below. Because of these limitations, the resulting hazard maps are useful for regional applications but should not be used as alternatives to site-specific studies in critical areas.

1) Every effort has been made to ensure the accuracy of the GIS and tabular components of the landslide inventory database, but it is not feasible to completely verify all original input data.

2) As previously discussed, the protocol is based on three primary data sets: a) landslide inventory, b) head scarp buffers, and c) additional geologic factors. The quality and completeness of these data sets, all of which have inherent uncertainty, can affect the level of detail and accuracy of the final deep landslide susceptibility map.

   - The landslide inventory data have limitations that are discussed in the protocol for inventory mapping of landslide deposits from light detection and ranging (lidar) imagery (DOGAMI SP-42 [Burns and Madin, 2009a]).
   - Calculation of head scarp buffers is limited based on the head scarp height (first buffer) and an average of the horizontal widths of previous or down slope blocks (second buffer). We assume that most large deep landslides have the potential to fail retrogressively upslope; however, this is not always the case.
   - The geologic factors to delineate in part the moderate susceptibility zone include susceptible geologic units, susceptible geologic contacts, susceptible slope angles for each engineering geologic unit polygon, and preferred direction of movement for each engineering geologic unit polygon. These factors are combined and a final score is produced. However, in some areas the delineation of the final moderate zone is based on visual overlap of these four factors; therefore, the accuracy and resolution of the output data can be overestimated or underestimated.

3) The GIS database is a "snapshot" view of current data; new information regarding landslides can be found or new landsliding may occur that could change the map.

4) Because the lidar-based digital elevation model (DEM) is only a model of elevation, it does not distinguish elevation changes that may be due to manmade structures like retaining walls. For a protocol and map intended to be used at the regional scale, it is not possible to conduct the extensive fieldwork required to locate all existing structures, determine the stability of each structure, and map each structure. Therefore, as a conservative approach, elevation changes not mapped as structures are assumed to be slopes; these must be examined on a site-specific basis.

5) Some landslide areas in the inventory may have been mitigated, thereby reducing their level of susceptibility. Because it is not feasible to collect detailed site-specific information on every landslide, potential mitigation has been ignored.

6) Prediction or estimation of displacement or runout of deep landslides is not included in maps produced following this method.

7.0   POTENTIAL USES OF DEEP LANDSLIDE SUSCEPTIBILITY DATA

The main purpose of this protocol is to provide a detailed explanation of the deep landslide susceptibility mapping process. Following the protocol ensures consistency in future maps produced by DOGAMI and by other practitioners and provides a technical reference for those maps. We intend these maps to provide useful information to guide site-specific investigations for future developments, assist in regional planning, and assist in mitigation of existing landslides and slopes.

Deep landslide susceptibility maps can serve as useful tools for differentiating areas of higher and lower hazards. This information is basic to emergency and land use applications. As an aid to emergency management activities the maps can be used for the development and refinement of emergency response plans and estimation of resource impacts from future landslide movement. Common applications of landslide susceptibility data in land use planning include input to comprehensive planning and the development of hazard ordinances with attached zoning and regulations. While the data and resulting maps are not appropriate for site-specific evaluations, they are valuable for regional screening for landslides and the selection of appropriate areas on which to focus further site-specific studies. The data and maps are particularly suitable for incorporation into state, county, and city hillside development ordinances.

8.0   ACKNOWLEDGMENTS

9.0   REFERENCES

Baum, R.L., Galloway, D.L., and Harp, E.L., 2008, Landslide and land subsidence hazards to pipelines: U.S. Geological Survey Open-File Report 2008-1164, 192 p . Web: http://pubs.usgs.gov/of/2008/1164/

Burns, W.J., 2014, Statewide Landslide Information Database for Oregon [SLIDO], release 3.2: Oregon Department of Geology and Mineral Industries, Web: http://www.oregongeology.org/sub/slido/

Burns, W.J., in press, Statewide Landslide Information Database for Oregon [SLIDO], release 4.0: Oregon Department of Geology and Mineral Industries.

Burns, W.J., and Madin, I.P., 2009a, Protocol for inventory mapping of landslide deposits from light detection and ranging (lidar) imagery: Oregon Department of Geology and Mineral Industries Special Paper 42. Web: http://www.oregongeology.org/pubs/sp/SP-42.zip

Burns, W.J., and Madin, I.P., 2009b, Landslide inventory map of the northwest quarter of the Oregon City quadrangle, Clackamas County, Oregon: Oregon Department of Geology and Mineral Industries Interpretive Map IMS-26, 1 pl, scale 1:8,000, GIS files. Web: http://www.oregongeology.org/pubs/ims/IMS-026.zip

Burns, W.J., and Mickelson, K.A., 2016, Landslide susceptibility overview map of Oregon: Oregon Department of Geology and Mineral Industries, Open-File Report O-16-02, 48 p., 1 pl., GIS file. Web: http://www.oregongeology.org/pubs/ofr/p-O-16-02.htm

Burns, W.J., Hofmeister, R.J., and Wang, Y., 2008, Geologic hazards, earthquake and landslide hazard maps, and future earthquake damage estimates for six counties in the Mid-Willamette Valley including Yamhill, Marion, Polk, Benton, Linn, and Lane Counties and the City of Albany, Oregon: Oregon Department of Geology and Mineral Industries, IMS-24. http://www.oregongeology.org/pubs/ims/p-ims.htm

Burns, W.J., Madin, I.P., and Mickelson, K.A., 2012a, Protocol for shallow-landslide susceptibility mapping: Oregon Department of Geology and Mineral Industries, Special Paper 45. Web: http://www.oregongeology.org/pubs/sp/p-SP-45.htm

Burns, W.J., Duplantis, S., Jones, C.B., and English, J.T., 2012b, Lidar data and landslide inventory maps of the North Fork Siuslaw River and Big Elk Creek watersheds, Lane, Lincoln, and Benton Counties: Oregon Department of Geology and Mineral Industries, Open-File Report O-12-07. Web: http://www.oregongeology.org/pubs/ofr/p-O-12-07.htm

Burns, W.J., Mickelson, K.A., Jones, C.B., Pickner, S.G., Hughes, K.L., and Sleeter, R., 2013, Landslide hazard and risk study of northwestern Clackamas County, Oregon: Oregon Department of Geology and Mineral Industries Open-File Report O-13-08, 38 p., 74 pl. Web: http://www.oregongeology.org/pubs/ofr/p-O-13-08.htm

Burns, W.J., Mickelson, K.A., and Stimely, L.L., 2014, Landslide inventory of coastal Curry County, Oregon: Oregon Department of Geology and Mineral Industries, Open-File Report O-14-10, 8 pl., scale 1:14,000. Web: http://www.oregongeology.org/pubs/ofr/p-O-14-10.htm

Burns, W.J., Mickelson, K.A., Jones, C.B., Tilman, M.A., and Coe, D.E., 2015, Surficial and bedrock engineering geology, Landslide inventory and susceptibility, and surface hydrography of the Bull Run Watershed, Clackamas and Multnomah Counties, Oregon: Oregon Department of Geology and Mineral Industries, Special Paper 46, 5 pl. http://www.oregongeology.org/pubs/sp/p-SP-46.htm

Christenson, G.E., and Ashland, F.X., 2006, Assessing the stability of landslides—Overview of lessons learned from historical landslides in Utah, 40th Symposium on Engineering Geology and Geotechnical Engineering 2006, Logan, Utah, http://files.geology.utah.gov/online/techrpt/lessons_learned.pdf

Dobbs, M.R., Culshaw, M.G., Northmore, K.J., Reeves, H.J., and Entwisle, D.C., 2012, Methodology for creating national engineering geological maps of the UK: Quarterly Journal of Engineering Geology and Hydrogeology, v. 45, no. 3. 335-347. doi: 10.1144/1470-9236/12-003

FEMA (Federal Emergency Management Administration), 2011, Hazus®-MH 2.1, Multi-Hazard loss estimation methodology, software and technical manual documentation. Web: http://www.fema.gov/media-library/assets/documents/24609?id=5120

Giraud, R.E., and Shaw, L.M., 2007, Landslide susceptibility map of Utah: Utah Geological Survey Map 228, 11 p., 1 pl. scale 1:500,000. http://geology.utah.gov/online/m/m-228.pdf

Godt, J.W., Schulz, W.H., Baum, R.L., and Savage, W.Z., 2008, Modeling rainfall conditions for shallow landsliding in Seattle, Washington, *in* Baum, R.L., Godt, J.W., and Highland, L.M., eds., Landslides and engineering geology of the Seattle, Washington, area: Geological Society of America Reviews in Engineering Geology, v. 20, p. 137–152.

Highland, L., compiler, 2004, Landslide types and processes, U.S. Geological Survey Fact Sheet 2004-3072 (ver. 1.1), 4 p. Web: http://pubs.usgs.gov/fs/2004/3072/

Hong, Y., Adler, R.F., and Huffman, G.J., 2007, Satellite remote sensing for global landslide monitoring, Eos, Transactions American Geophysical Union, v. 88, no. 37. doi: 10.1029/2007EO370001

Iverson, R.M., George, D.L., Allstadt, K., Reid, M.E., Collins, B.D., Vallance, J.W., Schilling, S.P., Godt, J.W., Cannon, C.M., Magirl, C.S., Baum, R.L., Coe, J.A., Schulz, W.H., and Bower, J.B., 2015, Landslide mobility and hazards: implications of the 2014 Oso disaster, Earth and Planetary Science Letters, v. 412, 197–208. doi: 10.1016/j.epsl.2014.12.020

Keaton, J.R., and Degraff, J.V., 1996, Surface observation and geologic mapping, *in* Turner, A.K., and Schuster, R.L., eds., Landslides: investigation and mitigation: Washington, D.C., National Academy Press, Transportation Research Board, National Research Council Special Report 247, p. 178–230.

Keaton, J.R., Wartman, J., Anderson, S., Benoît, J., deLaChapelle, J., Gilbert, R., and Montgomery, D.R., 2014, The 22 March 2014 Oso Landslide, Snohomish County: Geotechnical Extreme Events Reconnaissance (GEER) Association, Report GEER-036, 175 p. Web: http://www.geerassociation.org/administrator/¬components/com_geer_reports/geerfiles/GEER_Oso_Landslide_Report_low-res.pdf

Lane, J.W., 1987, Relations between geology and mass movement features in a part of the East Fork Coquille River Watershed, southern Coast Range, Oregon [M.S. thesis]: Oregon State University, 107 p. Web: http://ir.library.oregonstate.edu/xmlui/handle/1957/18455

Ma, L., Madin, I.P., Olson, K.V., Watzig, R.J., Wells, R.E., and Priest, G.R., compilers, 2009, Oregon geologic data compilation [OGDC], release 5 (statewide): Oregon Department of Geology and Mineral Industries Digital Data Series OGDC-5. [OGDC-5 superseded by OGDC-6; Web: http://www.oregongeology.org/pubs/dds/p-OGDC-6.htm]

Madin, I.P., and Burns, W.J., 2013, Ground motion, ground deformation, tsunami inundation, coseismic subsidence, and damage potential maps for the 2012 Oregon Resilience Plan for Cascadia Subduction Zone Earthquakes: Oregon Department of Geology and Mineral Industries, Open-File Report O-13-06. http://www.oregongeology.org/pubs/ofr/p-O-13-06.htm

Radbruch-Hall, D.H., Colton, R.B., Davies, W.E., Lucchitta, I., Skipp, B.A., and Varnes, D.J., 1982, Landslide overview map of the conterminous United States: U.S. Geological Survey Professional Paper 1183, 25 p., 1 pl. Web: https://pubs.er.usgs.gov/publication/pp1183

Roering, J.J., Kirchner, J.W., and Dietrich, W.E., 2005, Characterizing structural and lithologic controls on deep-seated landsliding: Implications for topographic relief and landscape evolution in the Oregon Coast Range, USA, GSA Bulletin; May/June 2005; v. 117; no. 5/6; p. 654–668. doi: 10.1130/B25567.1

Safran, E.B., Anderson, S.W., Mills-Novoa, M., Kyle House, P., and Ely, L., 2011, Controls on large landslide distribution and implications for the geomorphic evolution of the southern interior Columbia River basin, Geological Society of America Bulletin, v. 123, no. 9-10, p. 1851–1862. doi: http://dx.doi.org/10.1130/B30061.1

Santha-Mahlingham, R., Olsen, M.J., Sharifi-Mood, M., and Gillins, D.T., 2015, Landslide susceptibility analysis of lifeline routes in the Oregon Coast Range: DOGAMI Open-File Report O-15- 01. Web: http://www.oregongeology.org/pubs/ofr/p-O-15-01.htm

Sidle, R.C., and Ochiai, H., 2006, Landslides: processes, prediction, and land use: Washington, D.C., American Geophysical Union Water Resources Monograph 18, 312 p.

Spiker, E.C., and Gori, P., 2003, National landslide hazards mitigation strategy — a framework for loss reduction: U.S. Geological Survey Circular 1244, 56 p. Web: http://pubs.usgs.gov/circ/c1244/

Soeters, R., and van Westen, C.J., 1996, Slope instability recognition, analysis, and zonation, *in* Turner, A.K., and Schuster, R.L. eds., Landslides—Investigation and mitigation: Transportation Research Board Special Report 247, National Research Council, Washington, D.C., p. 129–177.

Turner, A. K., and Schuster, R. L., eds., 1996, Landslides: investigation and mitigation: Washington, D.C., National Research Council, Transportation Research Board Special Report 247, 673 p.

Varnes, D. J., 1978, Slope movement types and processes, *in* Schuster, R. L., and Krizek, R. J., eds., Landslides: analysis and control: Washington, D.C., National Research Council, Transportation Research Board Special Report 176, p. 11–33.

Wang, Y., Summers, R.D., and Hofmeister, R.J., 2002, Landslide loss estimation pilot project in Oregon: Oregon Department of Geology and Mineral Industries Open-File Report O-02-05, 23 p. Web: http://www.oregongeology.org/pubs/ofr/O-02-05.pdf

10.0 APPENDIX: GEOGRAPHIC INFORMATION SYSTEM (GIS) DETAILS

This appendix shows step-by-step instructions for creating the high landslide susceptibility zone and the preliminary moderate landslide susceptibility zone using Esri® ArcGIS® version 10.1 software. The user should have an intermediate level understanding of ArcMap® and Spatial Analyst®. The method we use combines several inputs, most of which are taken from deep landslide data extracted from a landslide inventory created by following the protocol described in DOGAMI Special Paper 42 (Burns and Madin, 2009a). Each input is assigned relative score value and then combined into a final dataset, which is used to assign areas of low, moderate, and high susceptibility. Recall that the contributing inputs are:

- for the high susceptibility zone (main text section **3.2**):
  - landslide deposits
  - head scarp-flank polygons
  - head scarp-flank polygon buffers
- for the moderate susceptibility zone (main text section **3.3**):
  - susceptible geologic units
  - susceptible geologic contacts
  - susceptible slope angles for each engineering geologic unit polygon
  - preferred direction of movement for each engineering geologic unit polygon
- low susceptibility zone (main text section **3.4**)
  - simply the areas on the map not covered by high or moderate susceptibility zones

We have color coded terms in this appendix to aid in following the instructions:
- Blue = File Name
- Green = Field Name
- Red = Process/Tool Name

The process requires a number of GIS files and a folder structure.

10.1 Set Up the Project

1. Create folders in your working drive with the following names:
   - A_Landslide_Deposits
   - B_Head_ScarpFlanks
   - C_Geologic_Units
   - D_Geologic_Contacts
   - E_Slopes
   - F_Directions
   - G_Minimal_Moderate
2. Extract all deep landslide deposits from the landslide inventory geodatabase created by following the protocol in DOGAMI Special Paper 42 (Burns and Madin, 2009a) and name the new set Deep_Landslide_Deposits; save the new file in the A_Landslide_Deposits folder.
3. Extract all deep landslide scarp-flank polygons from the landslide inventory deposits and name the new set Head_ScarpFlanks; save the new file in the B_Head_ScarpFlanks folder.

4. Create the Engineering_Geology file (see section **3.3**) and save it in the C_Geologic_Units folder. Add a field called Polygon_ID (type=integer) to Engineering_Geology.
5. Compute a slope map from the bare-earth DEM using the Slope tool and name the new file Slope.
6. Compute an aspect map from the bare earth DEM using the Aspect tool and name the new file Aspect.

10.2 Create the High Susceptibility Zone

10.2.1 Landslide Inventory

1. Add two fields to the Deep_Landslide_Deposits file: Relative (text field, 25 characters) and Relat_Susc (short integer).
2. Use the Field Calculator to assign these values to the fields: Relative = "High" and Relat_Susc = 3.
3. Convert the Deep_Landslide_Deposits polygons to a raster by using the Feature to Raster tool with the field = Relat_Susc and the cell size = 3. Save the raster into the A_Landslide_Deposits folder and name the raster High_deposits (values = 0, 3), where 3 = high deep susceptibility zones.

10.2.2 Head Scarp-Flank Polygons and Buffers

1. In the Head-ScarpFlanks file, add two fields: HS×2 (short integer) and Buffer (short integer). Attribute the HS×2 field with HS_HEIGHT field times 2. Attribute the Buffer field with the larger value from either the HD_AVE or the HS×2 field.
2. Create the buffer values file using the Buffer tool on the Head_ScarpFlanks file with distance set to "field" = Buffer, side type = full, and dissolve type = none. Name the output file Head_ScarpFlanks_Buffer.
3. Add two fields: Relative (text field, 25 characters) and Relat_Susc (short integer) to the Head_ScarpFlanks_Buffer file and save it in the B_Head_ScarpFlanks folder.
4. In the Head_ScarpFlanks_Buffer file, assign all buffered head scarps a Relative = "High" and a Relat_Susc = 3.
5. Convert the polygons to a raster by using the Feature to Raster tool with the field = Relat_Susc and the cell size = 3.
6. Save the raster in the B_Head_ScarpFlanks folder and name the raster High_HSBuffer (values = 0, 3), where 3 = high deep susceptibility zones.

10.3   Prepare Factor Layers

1. Create a minimal moderate buffer zone (main text section **3.3.1**) around the buffered head scarps and landslide deposits by using the Join Field tool to join the Buffer field from Head_ScarpFlanks_Buffer to Deep_Landslide_Deposits (**Figure 10.1**).

Figure 10.1.   Esri® ArcGIS™ v.10.1 Join Field tool interface.
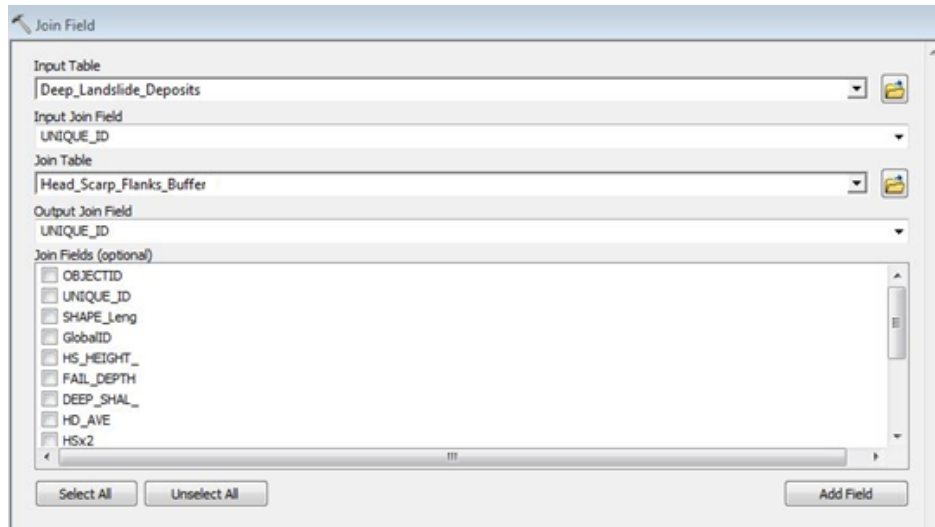
2. Export the Deep_Landslide_Deposits table: name the output file Moderate_buffer and save it in the G_Minimal_Moderate folder.
3. Copy all the features from the file Head_ScarpFlanks_Buffer to the file Moderate_buffer.
4. Use the Buffer tool on the Moderate_buffer file with field set to the Buffer, side type = full and dissolve type = all. Name the output file Moderate_zone.
5. Add two fields: Relative (text field, 25 characters) and Relat_Susc (short integer) to the Moderate_zone file and save it in the G_Minimal_Moderate folder.
6. Assign Relative = "moderate" and Relat_Susc = 2.

The rest of the moderate susceptibility zone is created through the combination of four factors. These factors are used to primarily determine the boundary between the moderate and low susceptibility zones. The four factors are:
- Susceptible geologic units
- Susceptible geologic contacts
- Susceptible slope angles for each engineering geologic unit polygon
- Preferred direction of movement for each engineering geologic unit polygon

These four factors will be turned into four raster datasets with scores ranging from 0 to 2 and then added together into a final moderate zone factors layer.

10.3.1 *Susceptible Geologic Units*

1. Save a copies of the Engineering_Geology and the Deep_Landslide_Deposits files into the C_Geologic_Units folder and name them Engineering_Geology1 and Deep_Landslide_Deposits1.
2. Run Dissolve on the Engineering_Geology file and then create a new field called Polygon_ID in the Engineering_Geology file and give every different unit a unique number (1, 2, 3, …). Finally, open the attribute table to confirm that the Engineering_Geology1 and Deep_Landslide_Deposits1 files are "exploded," because merged units will affect the spatial join.
3. Use the Union tool with the Engineering_Geology1 and Deep_Landslide_Deposits1 files and save the output as file Deep_Landslide_geopolys_union.
4. Run Dissolve on the Deep_Landslide_geopolys_union file.
5. Recalculate the areas.
6. Review that the correct engineering geology has been associated with each landslide. Make edits to the associated geology if necessary.
7. Use the Export to Dbase tool and save Deep_Landslide_geopolys_union in Excel format in the C_Geologic_Units folder.
8. Calculate the landslide area per unit area and convert to percent.
9. Add the field Score (short integer) to file Engineering Geology1. Assign all units scores as shown below:
    - Score = 0, if less 7%
    - Score = 1, if less than 17% and greater than or equal to 7%
    - Score = 2, if equal or greater than 17%
10. Convert the polygons to raster using the Feature to Raster tool with the field = Score and the cell size = 3. Save the raster into the C_Geologic_Units folder and name the file Geology (values = 0, 1, 2).

10.3.2 *Susceptible Geologic Contacts*

1. Create a blank Microsoft Excel spreadsheet called contact measurements with fields (column heads) called contact line name, LS Unique ID (landslide unique id), and Topological Left and Topological Right distances and save the Excel file in the D_Geologic_Contacts folder. This file will be used in a later step.
2. Save a copy of the Engineering_Geology1, Deep_Landslide_Deposits1, and ScarpFlanks files in the C_Geologic_Units folder and name the files Engineering_Geology2, Deep Landslide Deposits2, and ScarpFlanks2.
3. Use Engineering_Geology2 to select any two units with landslides located along their contact.
4. Run the Intersect tool with the two units selected. Output type = line.
5. Save the Intersect result as example file and name the file with the two unit names (for example, [unit name]_[unit name]_intersect) in the D_Geologic_Contacts folder.
6. Select all deep landslides from the Deep Landslide Deposits2 file and matching Head_ScarpFlanks file that touch or are close to (within a couple hundred feet [60 m] of the contact found in file [unit name]_[unit name]_intersect). Use these three files to make measurements (using the Measurement tool) up and down slope or, more importantly, on the topological right or left side of the contact line. Visually inspect the area on the topological right side of the contact to determine the location of the average distance from the contact to the head or toe of the landslide and use the measurement tool to find the distance value. See **Figure 10.2** for an example set of measurements.

Figure 10.2. Example distance measurements on the topological left and right of the contact.
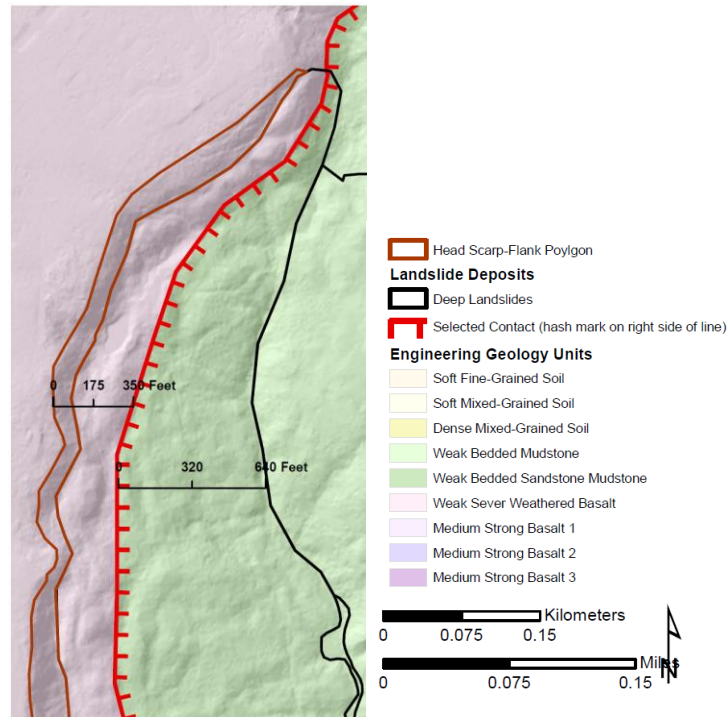
7. For each contact line or contact line segment, record the contact line name, LS Unique ID, and Topological Right and Topological Left distances in the contact measurements spreadsheet.
8. In the spreadsheet, calculate the mean and maximum for the topological right and left for each contact line (Table 10-1).

Table 10-1. Example recording of measurements along one contact.

Weak Sandstone + Medium Strong Basalt 1		
LS Unique ID	Topological Left	Topological Right
Dixie_Mountain_973	313	525
Dixie_Mountain_703	4800	3800
Dixie_Mountain_712	0	695
Dixie_Mountain_377	252	1349
Dixie_Mountain_230	66	1868
Dixie_Mountain_162	2689	1584
Dixie_Mountain_702	5300	1500
Dixie_Mountain_723	836	0
Dixie_Mountain_279	0	4336
Dixie_Mountain_700	1505	1270
Dixie_Mountain_100	1912	7289
Dixie_Mountain_217	555	185
Dixie_Mountain_249	53	276
Dixie_Mountain_788	234	387
Mean	1323	1790
Max	5300	7289

9. In ArcMap, use the Buffer tool to buffer each line on the right and left with the mean and maximum. This results in four buffers. Name the file with the two unit names as [unit name]_[unit name]_buffer and save the file in the D_Geologic_Contacts folder.

10. Use the Append tool to combine the two mean buffers (right and left). Use the Append tool to combine the two maximum buffers (right and left), then remove overlap. (If contacts overlap in Susceptible_Geologic_Contacts, use the Clip tool in the editor toolbar to clip the 1's out from underneath.)

11. Add the field Score (short integer) to the file [unit name]_[unit name]_buffer and save the file in the D_Geologic_Contacts feature dataset.

12. Assign all mean buffers a Score = 2 or a Score = 1.

13. Repeat for all susceptible contacts.

14. Use the Append tool to combine all the buffers into a single file and name the file Susceptible_Geologic_Contacts.

15. Add a polygon of the study area boundary to Susceptible_Geologic_Contacts.

16. Assign the boundary polygon a score of 0 and Clip the 1's and 2's (from step 11) from the boundary polygon.

17. Convert the polygons to raster using the Feature to Raster tool with the field = Score and the cell size = 3 ft.

18. Save the raster in the D_Geologic_Contacts folder and name the file Contacts.

### 10.3.3 Susceptible Slope Angles for Each Engineering Geologic Unit Polygon

1. Save a copy of the Deep_Landslide_geopolys_union file to the E_Slopes folder and name the file Deep_Landslide_geopolys_union3. Save a copy of the Engineering_Geology file to the E_Slopes folder and name the file Engineering_Geology3.

2. Run the Summary Statistics tool on file Deep_Landslide_geopolys_union3, with Output Table: eng_geol_slope_stats.dbf; Slope = Mean; Slope = STD; and Case Field = Polygon_ID (**Figure 10.3**).

Figure 10.3. Example of the Summary Statistics tool and settings.
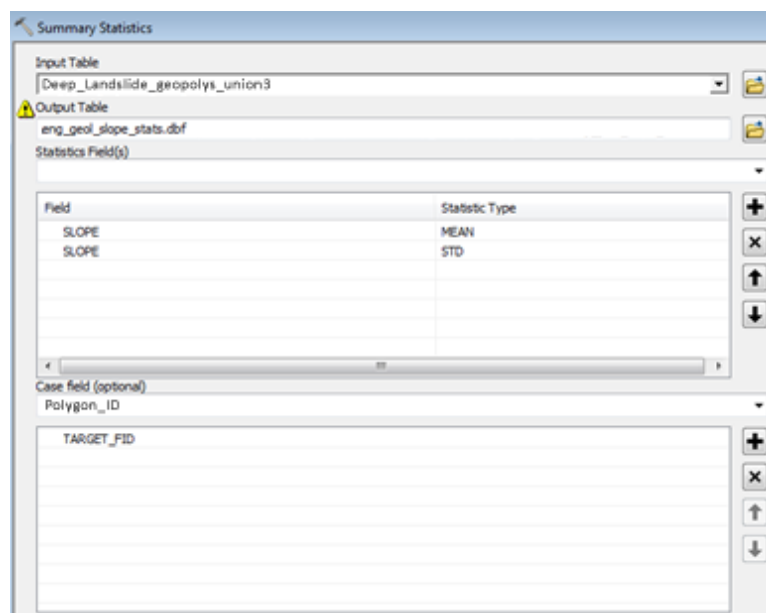
3. Use the Join Field tool to join eng_geol_slope_stats.dbf to Engineering_Geology3 using the Polygon_ID field (**Figure 10.4**).

Figure 10.4. Example of the Join Field tool and the settings.
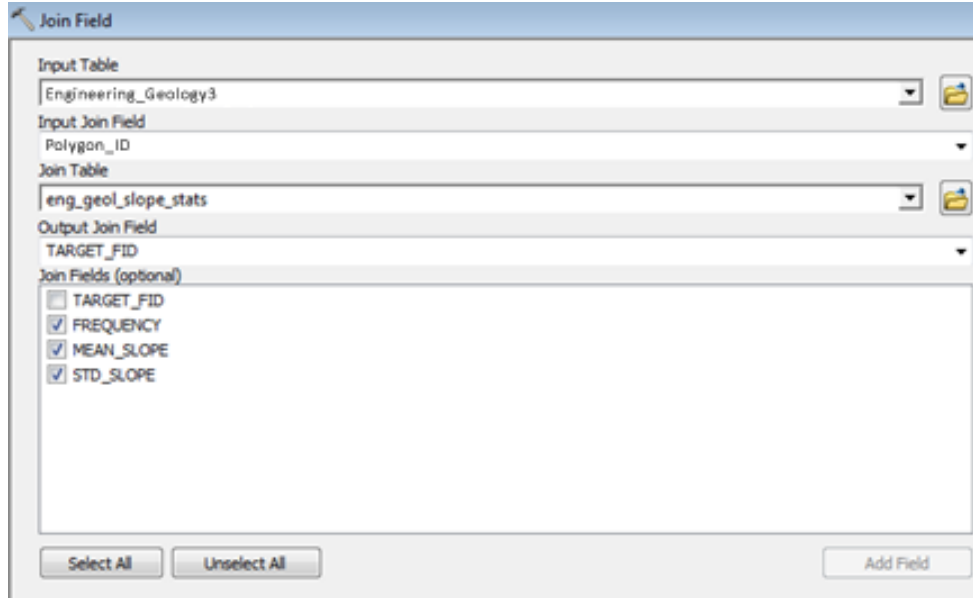
4. Add to the file Engineering_Geology3 two fields called Mean_1STD and Mean_2STD. Use the Field Calculator to calculate and populate field Mean_1STD with the mean field minus 1 STD and to calculate and populate field Mean_2STD with the mean field minus 2 STDs.
5. Convert Engineering_Geology3 to a raster using the Feature to Raster tool. Field is Mean_1STD = value. Output cell size is 3 ft. Name the Output Raster as Slope_Mean_1STD (0 to 90).
6. Use the Raster Calculator with equation Slope => Slope_Mean_1STD. Name the output raster Slope_High (0, 1). Use the Reclassify tool to turn value = 1 to value = 2 and leave value = 0; name the output raster file Slope_Highr.
7. Convert Engineering_Geology3 to a raster using the Feature to Raster tool. Field is Mean_2STD = value. Output cell size is 3 ft. Output Raster file name is Slope_Mean2STD (0 to 90).
8. Use the Raster Calculator with equation (Slope < Slope_Mean1STD) & (Slope > Slope_Mean2STD). Name the output raster file Slope_Mod (0, 1).
9. Use the Raster Calculator tool with equation Slope_Mod + Slope_Highr. Name the output raster file Slopes.
10. Use the Raster Calculator to reclassify any "no data" values to 0 and name the output file Slopes.
11. Next use the Focal Statistics tool with the "range" setting and a 100-ft^2 neighborhood. Name the output file Focal_100.
12. Use the Reclassify tool to reclassify the file Focal_100 file to (0, 1).
13. Use the Raster Calculator tool to multiply file Focal_100 with file Slopes, so that areas with less than 15 ft of relief (the 0 values) are removed from the Slopes file.
14. Save the raster in the E_Slopes folder and name the file Slopes.

10.3.4   Preferred Direction of Movement for Each Engineering Geologic Unit Polygon

1. Copy and paste the file Deep_Landslide_Deposits to the F_Directions folder and save the file as Deep_Landslide_Deposits4.
2. Dissolve the Deep_Landslide_Deposits4 polygons and create a 1,000-ft buffer file called 1000buffer.
3. Convert Deep_Landslide_Deposits4 to a raster using the Polygon to Raster tool and name the result Landslide_dir. Value = direction.
4. Convert raster cells to points using the Raster to Points tool with Value and name the result Landslide_Dir_points. Add any appropriate strike and dip points to this file and round the dip direction to 22.5 degree increments as specified in section 0 in the main text.
5. Create a TIN dataset with Landslide_Dir_points as the input point file with the direction selected as the elevation. Name the output file Points_Direction.
6. Convert the Points_Direction TIN file to a raster with 3-ft^2 cells and name the result Points_Direction2.
7. Use the 1000buffer file to delete areas greater than 1,000 feet from the landslides.
8. Use the Reclassify tool to reclassify the Points_Direction2 and Aspect values to the eight classes shown in **Table 10-2** and save the results as IDW_Direction_R (IDW = inverse weighted direction) and Aspect_R (**Figure 10.5**).

Table 10-2.   **Eight preferred directions of movement (aspect classes) after reclassifying.**

Old Value (degrees)			New Value	Compass Direction
Low	High			
–	0.000001	=	NoData	
−0.000001 –	22.5	=	**2**	**N**
22.5 –	67.5	=	3	NE
67.5 –	112.5	=	4	E
112.5 –	157.5	=	5	SE
157.5 –	202.5	=	6	S
202.5 –	247.5	=	7	SW
247.5 –	292.5	=	8	W
292.5 –	337.5	=	9	NW
337.5 –	360	=	**2**	**N**

Note that New Value 2 (bold text) appears twice in the table associated with two different degree ranges, which are combined into one compass direction, N.

Figure 10.5. Example of the Reclassify tool interface and settings.

9. Use the Raster Calculator to select all areas where IDW_Direction_R = Aspect_R and save as Direction_2.
10. Use the Reclassify tool to change any value 1 to 2 and retain any value 0 as 0 and save the result as Direction_2R. These will be the score = 2 areas.
11. Rename the files Aspect_R and IDW_Direction_R to Aspect and Direction, respectively, and use the Raster Calculator with the following equation (equation line breaks shown below are added for clarity here; do not use line breaks in the Raster Calculator tool) and save the file as Aspect_direction.

$$(("Aspect" == 2) \& ("Direction" == 3) | ("Aspect" == 2) \& ("Direction" == 9)) |$$
$$(("Aspect" == 3) \& ("Direction" == 2) | ("Aspect" == 3) \& ("Direction" == 4)) |$$
$$(("Aspect" == 4) \& ("Direction" == 3) | ("Aspect" == 4) \& ("Direction" == 5)) |$$
$$(("Aspect" == 5) \& ("Direction" == 4) | ("Aspect" == 5) \& ("Direction" == 6)) |$$
$$(("Aspect" == 6) \& ("Direction" == 5) | ("Aspect" == 6) \& ("Direction" == 7)) |$$
$$(("Aspect" == 7) \& ("Direction" == 6) | ("Aspect" == 7) \& ("Direction" == 8)) |$$
$$(("Aspect" == 8) \& ("Direction" == 7) | ("Aspect" == 8) \& ("Direction" == 9)) |$$
$$(("Aspect" == 9) \& ("Direction" == 8) | ("Aspect" == 9) \& ("Direction" == 2))$$

12. Create a file named Study_area_boundary and assign the boundary polygon a score of 0.
13. Clip the 1's (Aspect_direction) and 2's (Direction_2R) by using the Study_area_boundary.
14. Save the Aspect_direction file as Direction_1R. This file contains the score = 1 areas.
15. Use the Mosaic to New tool to create a new dataset by combining Direction_2R (2), Direction_1R (1), and Study_area_boundary (0), and name the result Direction file in the F_Directions folder.

10.4 Create the Preliminary Moderate Zone

1. Use the Raster Calculator to add the layers Geology + Contacts + Slopes + Direction and name file Moderate_Factors. Scores range from 0 to 8.

At this point, the protocol continues with an experienced geologist delineating the Moderate Susceptibility zone (see section 3.3.3 in the main text).